INVESTIGATION OF ARTIFICIAL LAKE DESTRATIFICATION--A HYDRAULIC MODEL STUDY

By

THOMAS ALAN GIBSON

Bachelor of Science

Oklahoma State University

Stillwater, Oklahoma

1972

Submitted to the Faculty of the Graduate College
of the Oklahoma State University
in partial fulfillment of the requirements
for the Degree of
MASTER OF SCIENCE
July 1974

INVESTIGATION OF ARTIFICIAL LAKE

DESTRATIFICATION--A HYDRAULIC

MODEL STUDY

Thesis Approved:

Robert M. Morelli
Thesis Adviser

W. A. Liederman

Dennis K. McLaughlin

N. N. Durham
Dean of the Graduate College

ACKNOWLEDGMENTS

The author wishes to express his appreciation to his major adviser, Dr. Peter Moretti, for his patient and invaluable guidance and assistance throughout this study, and to Dr. Dennis McLaughlin for his interest and assistance. The author would also like to express his gratitude to the many individuals whose contributions of time and advice helped immensely throughout the investigation. This project was funded by the Oklahoma Water Resources Research Institute.

TABLE OF CONTENTS

LIST OF TABLES

LIST OF FIGURES

NOMENCLATURE

g	gravitational constant
h	total depth
L	characteristic length
Re	Reynolds Number, $Re = UL/\nu$
Ri_1	Richardson number 1, $Ri = -g(\partial \rho/\partial z)/\rho_2(u/l)^2$
Ri_2	Richardson number 2, $Ri = -g(\partial \rho/\partial z)/\rho_2(u/w)^2$
Ri_3	Richardson number 3, $Ri = -g(\partial \rho/\partial z)/\rho_2(\dot{v}/v)^2$
t'	Non-dimensionalizing parameter
t^*	non-dimensional time $\frac{t}{t'}$
t	time
u	pump velocity
U	characteristic velocity
v	volume
$\dot{v}$	volume flow rate
w	horizontal characteristic length
y	vertical depth
z	vertical characteristic length

Greek Letters

Δ	difference
ν	kinematic viscosity
ρ	density
τ	non-dimensional time for complete destratification

Subscripts

h	Hamm's lake
m	model
w	water
a	air
t	tangential
p	perpendicular

CHAPTER I

INTRODUCTION

Artificial lake destratification is becoming an important method of water quality control. As far back as the late 1800's people in the United States have been trying to maintain good quality water in impoundments, but it has only been since the early 1950's that interest has arisen in the area of artificial lake destratification. Since that time artificial lake destratification has been shown to be an effective instrument of water quality control. The purpose of this experimental investigation was to determine the validity of a modeling technique as applied to mechanical lake destratification. The technique included the use of vertical scale exaggeration, in which the vertical and horizontal dimensions of the prototype are not reduced by the same amount. The horizontal dimensions of the prototype are reduced more than the vertical dimensions, thus producing an exaggerated vertical scale.

A real lake, on which destratification research has been conducted, is modeled in the laboratory and the results from the model are compared to the data acquired from the real lake. Chapter II examines the stratification phenomenon and the effects of artificial lake destratification on a lake and its biology while Chapter III introduces the real lake, the model, and the modeling parameters. Chapter IV discusses the entire experimental facility, including the methods and data used to determine the validity of the modeling technique, and

Chapter V presents the results.

Significance

The purpose of a lake destratification modeling technique is to carry out destratification research in the laboratory rather than in the field. By the use of a hydraulic model employing vertical scale exaggeration, the need for an extremely large model or for a costly and time consuming test on a real lake, is eliminated. The effects on a lake from the varying of one or more parameters can be economically studied in a model.

Background

There has been considerable research done in the area of modeling stratified flows using both analytical and hydraulic modeling techniques. However, literature dealing directly with lake destratification using either the hydraulic model or analytical tool is scarce.

One study done on vertical scale exaggeration in stratified flow was conducted in a previous research program by Vogel (26). The technique Vogel used to model the inflow into a stratified channel included the use of the Richardson number as the primary similitude parameter. This investigation uses the Richardson number as the primary similitude parameter, but modifies it to apply to mechnical lake destratification.

There is extensive literature in the field of thermal discharge into bodies of water and the mechanism of exchange flows in estuaries. Several analytical models of thermal effluent dispersion in large lakes have been collected into one work by Palicastro and Tokar (18). The

use of hydraulic models by Barr (1, 2, 3) to study exchange flows or by Francis (7) to model rivers and estuaries, including sand movements, are examples of the use of model simulation. Barr (1), in one of his papers, discusses the use of vertical scale exaggeration and the relevance of exchange flow studies to hydraulic model design, and in another paper, Barr (4) discusses the use and effects of different degrees of vertical scale exaggeration in hydraulic modeling.

More closely related to the topic of modeling lake destratification is the analytical model derived by Parsons (17) for temperature prediction in stratified lakes or the analytical model by Ligget and Kwang (14) to model the natural circulation in a stratified lake. The use of hydraulic models, in which no type of scale exaggeration was used, is discussed by Olds (16). Most of the models mentioned in the article by Olds are extremely large, with one model covering over 20,000 square feet. Hydraulic models of this size can be avoided by the use of an exaggerated vertical scale technique as in this study. Most closely related to this study is a work by Hogan, Reed, and Starbird (8) on mechanical aeration systems for rivers and ponds. In their work they have analytically described the process of mixing with different types of devices, but with the emphasis on aeration rather than mixing. No reports were found in the literature dealing explicitly with hydraulic modeling of mechanical lake destratification.

CHAPTER II

STRATIFIED LAKES

There are several effects on a lake related to artificial destratification. In this research study the modeling of the destratification process is the primary concern with any other effect which might occur due to the destratification considered secondary. However, in field research, many of these other effects are of primary importance. This chapter is intended to build an acquaintance with stratified lakes, explain the purpose for artificial destratification, and discuss some of the effects destratification has on a lake.

Effects of Destratification

When water is stored in lakes or reservoirs, it frequently stratifies during the summer season. The lake stratifies into three zones, the epilimnium, the thermocline, and the hypolimnium. The hypolimnium consists of cold denser water on the lake bottom while the epilimnium consists of the warmer and less dense top water. The thermocline is the area which separates the epilimnium from the hypolimnium. The lake in this condition is stable and the thermocline becomes a barrier across which there is little or no mass transport. Thermal stratification of reservoirs has been thoroughly reviewed by Kittrel (11) and a more detailed description of this phenomenon is presented there.

There is circulation in the epilimnium caused by wind or heating due to the sun. These currents carry the oxygen absorbed at the air-water interface throughout the epilimnium. Since there is very little or no mass transport across the thermocline, none of the oxygen-rich water of the epilimnium reaches the hypolimnium. Due to this phenomenon there is very little oxygen in the hypolimnium during periods of stratification. The oxygen that does reach the hypolimnium is quickly depleted because of the oxygen demand of the decaying material on the bottom. Through the years the material which does not decay, due to the lack of oxygen, collects on the bottom of the lake. This is one of the causes for the degeneration of a lake. The decaying material builds up because only slow, bad-smelling anaerobic processes continue in the absence of oxygen. There are other causes of lake degeneration which Brorchardt (5) discusses in an article on the causes and effects of lake degeneration and Task Group Reports by the American Water Works Association (29, 30, 31) detail the roll of nutrients in the degeneration process and water quality. The dissolved oxygen versus depth curves for Hamm's Lake, Figure 1, illustrates the oxygen deficiency in the hypolimnium and the increase of dissolved oxygen during mixing. The destratification of lakes is accomplished by mixing the hypolimnium and epilimnium together, giving a uniform temperature profile. In the process of destratification the oxygen in the epilimnium is introduced into the hypolimnium through mixing, thus providing oxygen for the decaying matter on the bottom.

The predominate type of algae in lakes during the summer season is blue-green algae. The bloom of this algae are often the cause of taste and odor problems in water supplies. Although it has not been

proved, it is believed that the cooling of the surface water, caused by destratification, produces a decline in the blue-green algae population and the predominate strain becomes the green algae type. The green algae is more advantageous to the lake biology. Articles by Symons et al. (21), and Teerink and Martin (25) discuss the effects of artificial lake destratification on plankton populations.

There are many references to the term a lake "turning over". This happens during late summer when a cool period makes the surface water cooler, and thus heavier, than the bottom water. The now heavier top water sinks to the bottom while the bottom water, and some of the decaying material on the bottom, is brought to the top. This results in extreme turbidity, odor, and taste problems for municipalities using a water supply affected by this phenomenon. Again, lake destratification will prevent this from happening by keeping the lake mixed all season, and preventing the decaying material from building up. There are many other benefits derived from lake destratification but there are also problems. Effects on fish due to the change in water temperature, increased turbidity due to the initial mixing, and adverse changes in the aquatic populations are some of the problems encountered when a lake is destratified. Papers by Churchill (6), Love (15), and Woodward and LeBosquet (27) discuss the benefits and problems of artificial lake destratification and the reader is referred to these references for additional detail.

Field Research

One of the first experiments in lake destratification was conducted by Hooper, Ball, and Tanner (9) in 1952. A mechanical device

was used to pump the water from the bottom to the top. They reported only partial success, but did manage to lower the thermocline relative to the surface. Since that date there have been numerous research projects on real lakes.

The research on lake destratification has not been limited to any one location. Research by such people as Knoppert et al. (12), in Rotterdam, are indicative of the world-wide interest in lake destratification. The most notable research work being done in the United States has been done by Symons et al. (21, 22, 23, 24). Work by Symons, beginning in 1964, has added knowledge on the running conditions, results, and effects on real lakes from destratification. An overall view of the concept of lake destratification with comparative results from several lakes is presented in a committee report on lake destratification by the American Water Works Association (28).

CHAPTER III

MODELING TECHNIQUE

This chapter is intended to present the reference lake used in this study along with the details of the model construction. The modeling parameters, such as the scale factors, similarity considerations, non-dimensional numbers, and particularly the Richardson number along with other modeling parameters are discussed in the latter part of this chapter.

Prototype

The ability of a modeling technique to model a real lake could probably best be measured by comparing the results of the model to data obtained from a real lake. Hamm's lake, a small lake five miles west of Stillwater, Oklahoma, was chosen as the lake to be modeled in this study. Hamm's lake was chosen because of its convenient location and because there was a destratification research project in its final stages being conducted on the lake at the time of this investigation.

The researcher forced the lighter top water, containing considerably more oxygen than the bottom water, downward to mix with the hypolimnium. The researcher then recorded temperature and dissolved oxygen profiles at different times during the destratification process. An illustration of the temperature profiles is presented in Figure 2. The type of algae and the turbidity of the water were also recorded.

The lake is a man-made lake and was built with the assistance of the Soil Conservation Service of the United States Department of Agriculture in 1964. The lake channel bottom was 905.6 feet above sea level when the lake was created, and the principle spillway is 941.6 feet above sea level. The change in depth of the lake due to silting since it was created has not been determined. The surface area of the lake is 99 acres and the volume is 919 acre feet. A small map of the lake is presented in Figure 3.

A propeller connected by a shaft to a one-half horsepower electric motor was used to force the top water downward. The propeller was enclosed in a cylindrical housing and the entire device was supported by a raft. The velocity of the water leaving the pump was measured by a screw type current meter placed beneath the propeller. The pumping device and its performance are presented in a paper by Quintero and Garton (20). In the paper by Quintero and Garton, a 15 foot long circular cone was suspended beneath the propeller to act as a diffuser. However, the cone was not used during the acquisition of data used in this study. A sketch of the pumping device with the cone is presented in Figure 4.

Model

The model was built in two different stages. The first stage was its basic construction in a box shape for the purpose of studying the general mechanism of lake destratification and the pump jet penetration of the thermocline. The second stage was the construction and installation of a contour, using the technique of vertical scale exaggeration.

The base of the model was constructed of a frame made out of 2 x 4 inch lumber with three sheets of one-half inch plywood, each 4 x 8 feet,

screwed down onto the frame. The plywood was then sealed by a layer of polyester based resin and fiberglass to give an 8 x 12 foot base. Another coat of polyester resin was laid down to obrain a smooth finish. The bottom was then painted with a polyester based epoxy white paint. The sides were made of one-half inch plexiglass to allow observation of the flow patterns. The eight foot ends were single sections of plexiglass 16 inches high. Without the availability of plexiglass sheets any longer than eight-feet, the twelve foot sides were constructed of two sections connected and reinforced by a splice. Sections of 2 x 4 inch lumber were grooved their entire length on the flat side and fitted over the plexiglass edge on top of the tank to keep the sides from bending out. The plexiglass was attached to the fiberglass and plywood bottom with brass screws placed every two inches. Silicone rubber sealer was used to seal any gaps between surfaces making contact with each other. A sketch of the model is included in Figure 5. A two inch stainless steel drain was placed in one corner of the tank and sealed in with silicone sealer. It was connected underneath the tank to one and one-half inch P.V.C. pipe which emptied into a drainage channel.

After several runs, in which the equipment was tested and observations were made and recorded, the contour was installed into the tank. Hamm's lake has many fingers which are not deep; these fingers were molded in sections and then placed in the tank and connected together. A male die of a section of a finger was reproduced using modeling clay with the aid of a contour map. An enclosure was made around the male die and then concrete was poured over the die. In this way the fingers of the lake were made in sections. The main body of the lake was too large to produce by the previous procedure and was therefore built

directly into the tank. A 2 x 12 inch retaining frame, which enclosed the main body of the lake, was built into the tank. Sand was filled into this enclosure and the contour was then shaped into the wet sand. The top one-half inch of sand was left off and a one-half inch coating of concrete was laid over the sand contour. The fingers were then placed in the tank, connected, and leveled to the proper height. The contour was painted with a polyester based epoxy white paint and the seams between the fingers were sealed with silicone rubber sealer. The dam portion of the lake was placed at one end of the tank, next to the plexiglass, allowing visual observation of the main body of water. A one and one-half inch section of P.V.C. pipe was built into the contour and connected to the original drain pipe. A photograph of the contour is included in Figure 6 and a curve of depth versus volume is included in Figure 7.

The pumping device for the model was designed from the prototype pumping device on Hamm's lake. The models pumping device was run by a direct current automobile heater fan motor powered by a variable voltage direct current power supply. The motor was mounted on a platform which could be suspended at any point in the model. A cylindrical housing, which encloses the propeller, was suspended down from the platform on which the motor was mounted. A three bladed propeller was cut from one-eight inch plexiglass and the three blades were twisted to produce an angle of about 30 degrees from the plane of the propeller hub. The propeller, which was one and one-quarter inch in diameter, was attached to the motor by a one-quarter inch brass shaft. Stator vanes were placed in the top of the cylindrical propeller housing to reduce the rotation of the fluid. Sketches of the pumping device and the carraige

are included in Figures 8 and 9.

The velocity of the water leaving the pump is measured by the use of an inverted manometer. The manometer uses air on water as the working fluids. A sketch of the manometer is presented in Figure 9 and a derivation of the equation used to find the velocity is included in Appendix B. The manometer and probe were later removed so their presence would not disturb the flow further downstream. A small magnet and counterbalance were attached to the propeller shaft above the water line. A wire coil was attached next to the shaft and the ends connected to an oscilloscope or counter. This apparatus allowed measurements of the revolutions per second of the shaft with the motion of the magnet producing changing lines of flux. A plot of velocity (as measured by the manometer) versus the revolutions per second allowed determination of velocity from shaft revolutions. The velocity calibration curve is presented in Figure 10. The uncertainty bands are discussed in Appendix G.

Modeling Parameters

The modeling of fluid flow situations is usually accomplished by making the ratios of the important forces in the real situation and those in the model the same. It would be better if the ratios of all the forces in the real situation and the ratios of the forces in the model could be made equal. However, this is not always possible. With both the horizontal and vertical scale factors in the model used in this study the same, where scale factor is defined as the ratio of real lake dimensions to model dimensions, the lake model would be on the order of one inch deep. When the destratification process is modeled using the Reynolds number, which is the ratio of the inertia forces to the viscous

forces and can be written as

$$Re = \frac{UL}{\nu} \quad , \tag{3-1}$$

the kinematic viscousity for both the real lake and model would differ by only 2% of the real lake value, and only the velocity and the characteristic length could change. The modeling would then require that

$$U_m L_m = U_h L_h . \tag{3-2}$$

With a scale factor of 360:1, equation (3-2) would require a model pump velocity of 360 times the Hamm's lake velocity, or 878 feet per second. This large a velocity cannot be used due to surface effects which are discussed later. It is not necessary and often acceptable to allow the Reynolds number in the model to be low if the flow regime remains the same, but while varying the velocity to obtain a practical value, the models Reynolds number would differ from the Hamm's lake Reynolds number more than two orders of magnitude. The shallowness of the model and the inability to obtain Reynolds numbers with less than an order of magnitude difference, suggest the use of vertical scale exaggeration as a technique to model artificial lake destratification. If the vertical scale is exaggerated then the vertical characteristic length of the model is increased, eliminating the extremely shallow model and producing a situation in which the Reynolds number, based on depth, of Hamm's lake and the model can be more closely matched. In this investigation, a vertical scale factor of 33.6:1 was obtained after the exaggeration and the horizontal scale factor was 360:1. With a vertical scale factor of 33.6:1, equation (3-2) would now require a velocity of 33.6 times the Hamm's lake velocity. Now a velocity on the order of one to two feet per second can be obtained while producing a difference in the Reynolds

numbers only slightly greater than one order of magnitude.

This study is not attempting to model a situation where the surface phenomenon is important, making the Froude number an unimportant parameter. It was necessary, however, to insure that surface phenomena did not affect the process being modeled. The primary concern was avoiding model pump velocities which would create a surfac depression allowing air to be entrained into the propeller. This condition places a limit on the velocities used because if the limit is reached, air will be entrained into the propeller. An analysis to determine the ideal maximum pump velocity while avoiding surface depression problems is presented in Appendix C.

Another non-dimensional parameter important in modeling free surface hydraulic models is the Richardson number. The derivation for an incompressible fluid is given by Prandtl (19) and leads to

$$Ri = \frac{(g/\rho)(\partial \rho/\partial z)}{(\partial u/\partial z)^2} . \qquad (3\text{-}3)$$

If a characteristic length is chosen over which the velocity and density vary, an overall form of the Richardson number can be obtained,

$$Ri = - \frac{(g/\rho)(\Delta\rho/z)}{(u/z)^2} . \qquad (3\text{-}4)$$

A derivation of this model law from both energy and elementary mass considerations is presented in detail by Vogel (26), and its use is discussed by Barr (1) and Francis (7).

The manner in which the terms in the Richardson number are defined will determine the accuracy with which the destratification process can be modeled since different horizontal and vertical scale factors were used. Some decision must be made as to which velocity and length should

be used in the Richardson number. As an example, there are several choices from which the characteristic length could be selected, such as lake width or depth.

Since destratification is accomplished by imparting energy, in the form of velocity to mix the lake, the most obvious choice for a characteristic velocity would be the jet velocity leaving the pump, since the destratification process is strongly dependent upon the penetration of the thermocline by the jet. Hence, the pump velocity was chosen as the characteristic velocity to be used in the Richardson number. Again, since the mixing process is dependent upon the penetration of the thermocline, the density difference through some characteristic length is chosen as the maximum density difference over the vertical height through which it varies. This value is simply read off the density profile curves. The last value in the Richardson number which is needed is a characteristic length over which the velocity varies. In this case two choices are evident, the depth of the lake or some horizontal dimension of the lake. If the velocity divided by characteristic length is considered as a group, one more value can be found for the Richardson number. The dimension of velocity divided by length is sec^{-1}. Another group of values which also has this dimension, and which would be characteristic of the lake, is volume flow rate divided by volume.

The prior reasoning produces three forms of Richardson number, where each Richardson number can be considered a non-dimensional velocity. Any given velocity can be non-dimensionalized by one of the methods described above, thus producing three non-dimensional velocities for each measured velocity. The experimental design provides for the ability to vary the velocity in order to find the velocity which would produce similar re-

sults in the model if the appropriate non-dimensional parameter were used. The three forms are summarized below:

$$Ri_1 = \frac{-g\left(\frac{\Delta\rho}{z}\right)}{\rho_2\left(\frac{u}{h}\right)^2} \tag{3-5}$$

$$Ri_2 = \frac{-g\left(\frac{\Delta\rho}{z}\right)}{\rho_2\left(\frac{u}{h}\right)^2} \tag{3-6}$$

$$Ri_3 = \frac{-g\left(\frac{\Delta\rho}{z}\right)}{\rho_2\left(\frac{\dot{v}ol}{vol}\right)^2} \tag{3-7}$$

where: g is the gravitational constant and is equal to 32.2 ft/sec^2

$\frac{\Delta\rho}{z}$ is the maximum density difference divided by the height through which it varies

ρ_2 is the heaviest or bottom density of the lake or model

u is the velocity of the jet leaving the pump

h is the water height of the lake or model

w is the width (or length) of the lake or model

$\dot{v}$ is the flow rate of the pump

v is the volume of the lake or model

Subscripts h and m will be used to refer to Hamm's lake and the model respectively.

Since the primary purpose of lake destratification is to mix two volumes of water together, the hypolimnium and the epilimnium, then the volume of water contained in the lake will be a determining factor in the time it takes to destratify the lake. Therefore, in placing the contour in the rectangular box, any part of the lake left out would delete the total volume of water in the model. By picking a suitable horizontal scale factor, as that chosen, it was made possible to place

the entire contour into the rectangular box, thus leaving out no volume of water. A horizontal scale factor of 360:1 was chosen and this will help alleviate any discrepancies due to any volume of water which might have been left out. It was necessary, however, to curve the fingers of the lake in order to fit them into the box. This will not produce any noticeable error in the results since the volumes being mixed are the variables of primary importance.

The vertical scale factor was chosen as 33.6:1. As was mentioned previously, this scale factor allows the models pump velocity to be varied while the models Reynolds number and the Hamm's lake Reynolds number remain within an order of magnitude of one another. The total depth of the model for a scale factor of 33.6:1 is 10.25 inches.

The pumping device itself was scaled using the vertical scale factor. Since the modeling will not be exact, expecially due to the difference in scale factors, several compromises must be made such as the Reynolds number variation. The pump was scaled using the vertical scale factor in order to produce local similarity near the pumping device. The lake cannot be exactly modeled both near the pump and far away from the pump, but since the mixing (near the pump) is the phenomenon of the most interest, and strongly influences destratification rates, modeling near the pump is given priority.

Prediction of the time necessary to destratify a real lake could be an invaluable tool in water quality control. However, trying to determine the appropriate Richardson number and also an appropriate time scale produces two unknown parameters. There may be more than one pair of apparently successful parameters. In this investigation an attempt was made to find a pair of parameters, a Richardson number and

a time scale, which would produce the closest similarity when used together. The mixing rate of the pump divided by the total volume of fluid that needs to be mixed would result in a parameter having the dimension of time. Such a parameter, involving both the mixing rate and total volume to be mixed, includes two characteristics of the lake. It is this parameter, having the dimension of time, which will be used to provide a non-dimensional time scale for lake destratification. An important parameter would be the non-dimensional time needed to destratify a lake. The following parameters will be defined for later reference:

t time

t^* non-dimensional time

t' non-dimensionalizing parameter $(v/\dot{v})$

τ non-dimensional time needed for complete destratification

The ability of the modeling technique presented in this chapter to model artificial lake destratification will be based on two sets of criteria. The first set will be the comparison of density profiles taken from Hamm's lake and those recorded in the model. The second set will be the ability of a given pair of parameters, a Richardson number and the non-dimensional time presented above, to model the real lake.

CHAPTER IV

EXPERIMENTAL TECHNIQUE

The experimental facility is presented in detail in this chapter along with the procedure used for individual runs. The data collection technique and procedure used to reduce the data are also presented.

Experimental Facility

The construction of the lake model and the contour were presented in Chapter III. This section is intended to present the entire facility used for the research.

The tank is supported by concrete blocks and the bottom of the tank is one foot above the floor. A grid was placed on the side of the tank, using one-sixteenth inch black circuit tape, to aid in the visual observation of the flow, and a new grid was placed on the end of the tank when the contour was built. The DC power supply was placed on a table at one end of the tank. The salt needed to produce the desired density difference for each run was mixed with water in a 45 gallon tank placed on top of a table. A tee with ball valves in each tee was connected to the fresh water supply. One tee was connected to the 45 gallon tank by garden hose while the other branch of the tee was connected to a garden hose with one free end.

A dye injection system was constructed to enable a visual inspection of the flow. A plexiglass cylinder, 10 inches high with a three inch

diameter, was fastened on a movable platform mounted on the 2 x 4 inch frame on the top of the tank. A six foot tube of one-eighth inch plastic was connected to a small ball valve fitting on the bottom of the dye pot. The plastic tubing was fitted with a large hypodermic needle which was positioned over the propeller housing where the dye was mixed into the flow by the propeller. With the motor platform movable both vertically and horizontally, the pump could be placed at any location in the lake model. A sketch of the entire facility is presented in Figure 11.

Data Collection

One of the two data collection systems was a conductivity probe used to measure density. The probe was constructed of 0.002 inch platinum wire with one end sealed in three millimeter flint glass tubing. The flint glass tubing was heated and stretched to produce an elongated tip. The platinum wire was then placed into the elongated glass tubing and the glass then melted around the tip of the wire to seal the tip of the probe. The other end of the platinum wire was connected to electrical wire encased in five millimeter flint glass tubing. The blunt end of the three millimeter glass tubing, in which the platinum wire was encased, was fastened into the end of the five millimeter glass tubing. The tip was then coated with a platinum black solution. A plexiglass stand was made in which the conductivity probe could be placed and its height varied. The conductivity circuit was made up of the probe and a wire mesh which were both placed in the fluid with the other ends of each connected to a Wheatstone resistance bridge. A sketch of the probe and its circuit are included in Figure 12. A calibration curve for the conductivity probe was made by plotting the resistance versus the

specific gravity for several known salt solutions. The density profile of the model could then be determined for any situation by recording the resistances for several depths and using the calibration curve to find the specific gravity. A typical calibration curve is presented in Figure 13.

The second data collection system was a photographic arrangement to record the flow patterns made visible by the dye. The center line of the grid was centered on the side of the tank with the vertical grid lines placed every six inches out from the centerline. The horizontal grid lines were placed every two inches beginning two inches above the bottom of the tank. A 135 mm Minolta Hi-Matic 9 rangefinger camera with f 1.7 lens was used to photograph each run. The camera was placed on a tripod 75 inches from the side of the tank. The center of the lens was placed on the same level as the six inch grid line above the tank bottom. The camera was placed in the same position each time for consistency so the photographs could be compared from one run to another. Both Kodak Plus-X Pan and Kodak Tri-X Pan black and white film were used with the Tri-X Pan used the majority of the time due to the need for less light with this film. The lighting for the rectangular tank was obtained from the regular overhead florescent lights and four lights placed just below the water line. Two 500 watt photographic flood lights were placed in back of the tank just inside the corners and below the water line and two 300 watt service lights were placed in front of the tank just inside the corners and below the water line. Both green and red food coloring was used to dye the fluid with the green dye providing the best photographic contrast. A mount for the camera was also constructed in the ceiling of the lab to provide a means of photographing the

fingers of the lake when the contour was placed in the tank. The lighting with the contour in place consisted of one 500 watt photographic light placed above and behind the main body of the lake and pointing down into the water at a 30 degree angle.

Data Reduction

The maximum initial density difference in Hamm's lake was 62.1877 lbm/ft^3 to 62.3749 lbm/ft^3. This produces a density difference of 0.1872 lbm/ft^3. This small a density difference used in the Richardson number requires very small velocities to be used in the model which are extremely hard to measure and produce large errors in reading the Δh from the pitot tube. To acquire better accuracy some procedure was needed to make use of the much larger density difference obtainable by the use of salt. The equation below used a characteristic of the Hamm's lake curve, the maximum density difference, to determine the densities to be used in the model.

$$\rho_{ym} = \frac{(\rho_y - \rho_1)_h}{a(\rho_2 - \rho_1)_h} + \rho_{1m} \qquad (4\text{-}1)$$

The subscripts 1 and 2 refer to the density of the top and bottom water respectively. The y subscript indicates the vertical point which is being converted from one curve to another. The a is an arbitrary constant which determines the maximum density spread for the model. If a is equal to one, the maximum density spread will equal 1 lbm/ft^3. As a increases the density spread decreases and as a decreases the density spread increases.

The density of the water in the model, measured with the use of the conductivity probe, was plotted as a function of depth. The resulting density curve was reduced by the above procedure and a comparison of the Hamm's lake density curve and the models density curve could be made.

An attempt was made to produce a model density curve that, when reduced by the above equation, would have the same surface and bottom density points as the Hamm's lake curve and whose departure from the constant density of the surface occurred at the same point as the Hamm's lake curve. Also, an attempt was made to produce a reduced model density curve where the slope of the curve where the maximum change in density per depth occurred had the same value as the slope of the Hamm's lake curve at the corresponding point.

The penetration of the thermocline by the pump jet was determined by observing the dyed part of the jet with respect to the grid pattern on the tank. An estimate of the depth penetrated by each velocity used in the Richardson numbers could be obtained by the above procedure. The growth of the lens was also determined by observing its width as measured by the grid pattern.

The center of gravity of a lake which is being destratified, moves upward from a given datum as the destratification continues. This provides another tool which might prove useful in modeling a lake. If the temperature or density profile, and the volume or surface area for several heights are known, the lake can be subdivided into several sections. The weight of each section can be calculated knowing the density and volume. An arbitrary datum point is selected and the first moment of area of each section is found and the sum of the first moments is divided by the sum of the sections weights. This gives the center of

gravity above the chosen datum. The average density can be calculated by dividing the sum of the sections weights by the total volume of the lake.

The center of gravity for the mixed lake can be computed by the above procedure knowing the average density. With the center of gravity for both the stratified lake and the mixed lake known, the energy required to lift the center of gravity of the stratified lake can be determined. Again choosing an arbitrary datum point, the potential energy of the lake in both conditions can be found by multiplying the weight of the lake by its moment arm. The difference between the potential energy of the lake in the stratified and mixed condition produces the theoretical amount of energy required to destratify the lake. This is only the theoretical amount since it does not account for energy losses due to mixing or pump inefficiency. If profiles have been taken over a period of time, a curve of the remaining energy required to destratify the lake versus time can be plotted. If some type of correlation could be found between the potential energy versus time curve for a real lake and a model, another useful tool could be added to modeling lake destratification. The potential energy curves for Hamm's lake and the model were studied in this investigation. The volume for every four feet of depth was known as was the temperature profile. The type of numerical calculations described previously are easily adaptable to computer programming. A program was written to perform the calculations needed to plot a potential energy curve, and is included in Appendix D. The program was written for a Hewlett Packard 9820A desk mini-computer with a plotter. The results obtained from the potential energy curves are discussed in Appendix F.

Experimental Procedure

The first step for each run for both the rectangular tank and the contour was establishing the desired initial conditions. Fresh water was introduced into the tank until some specified height was reached. Salt was mixed with water in the overhead tank until the specific gravity desired was obtained. The end of a connecting hose was then placed in the tank and the salt water from the overhead tank was introduced into the lake very slowly. Three to four more tanks of salt water were added to obtain the final desired height of water. A different initial profile could be obtained depending on the exact procedure followed and the specific gravity used in the overhead tank.

After several attempts, the appropriate procedure needed to reproduce the desired density profile in the model was found. The resulting curve, with density as a function of depth, was similar to the Hamm's lake density curve. The procedure consisted of filling the tank with fresh water to a height of 6.5 inches. The first tank of salt water, with a specific gravity of 1.028, was run in at 0.5 gallons per minute with the garden hose placed parallel and on the bottom of the lake. The next four tanks, with specific gravities of 1.030, 1.0315, 1.033, and 1.035 respectively, were run in at 0.15 gallons per minute with the garden hose perpendicular and one-half inch from the bottom of the lake. The model was allowed to settle one to two hours after reaching the final height of 10.35 inches in order to let any currents be damped out.

The profile of the lake was taken using the conductivity probe. Readings were taken in one-half inch increments beginning at the top of the lake. The profile was plotted and the desired velocity was then

calculated. After the lights, camera, and a clock were positioned the pump was started and the velocity brought up to its proper value. The dye was released and pictures were taken the first 30 to 40 seconds to record the jet penetration of the thermocline and initial lensing. Four to six pictures were taken during the next 30 minutes to determine if the lens grew to the top or bottom. The pump was stopped and measurements were again taken with the conductivity probe. The resulting curves of density as a function of depth allowed the calculations needed to produce a potential energy curve. With the contour in place pictures were taken the first 20 to 30 seconds to record the jet penetration and then the camera was placed about 10 feet above the fingers of the lake to record the progress of the dyed lens into the fingers. Profiles were taken at a location determined through scaling from Hamm's lake, and at two positions in the fingers of the contour to determine the extent of penetration of the salt lens into the fingers.

CHAPTER V

RESULTS AND DISCUSSION

As has been previously discussed there were two sets of experiments. The first set consisted of observations of the general mechanism of lake destratification and the jet penetration of the thermocline. The second set of data was collected with the contour in place. The density profiles to be compared to those of Hamm's lake were obtained during this second set of experiments and the time for total destratification of the model was recorded. The importance of the volume of water in the fingers was not evident at the beginning of this investigation and the penetration of the mixing lens into the fingers was an important observation of the second series of experiments.

Destratification Process

Basically, three groups of experiments were conducted in this first series of experiments with each group related to one of three Richardson numbers. The same density profile, similar to the profile of Hamm's lake, was duplicated for each Richardson number. Figure 14 presents the initial Hamm's lake density curve with the reduced model curve superimposed on it. The surface and bottom density points correspond and both curves depart from the density of the surface water at the same point. Also, the slope of the curve where the maximum change in density per depth occurs, has the same value as the corresponding slope on the

Hamm's lake curve. Under the above conditions, the momentum of the jet in the model must penetrate a similar density barrier as the jet in the real lake. Matching Ri_1, Ri_2, and Ri_3 with Ri_h produced the highest velocity with Ri_1, an intermediate velocity with Ri_2, and the smallest velocity with Ri_3. Table I in Appendix E lists the values for one particular series of experiments conducted in the rectangular tank.

It was expected that when the top water was mixed with the denser lower water, an intermediate density fluid would result and seek its own level due to buoyant and gravitational forces. This was confirmed in the first series of experiments, but the primary observations were the jet penetration of the thermocline and the growth of the lens.

The density range obtainable from the use of salt was 62.46 lbm/ft^3 to 64.9 lbm/ft^3. To obtain high enough velocities to be easily measurable, densities as high as 64.58 lbm/ft^3 were used. These high salt concentration solutions produced extremely hazy bottom layers of fluid which made it very difficult to determine the jet penetration accurately. The maximum density difference for a specified interval of the profile was considered the barrier which the jet needed to penetrate. In Hamm's lake the maximum density difference occurred between 13 feet and 16.5 feet below the surface of the lake, which corresponds to a depth of between 4.69 inches and 5.85 inches in the model. The minimum penetration observed for all three velocities was at least four and one-half inches. This is on the very edge of the thermocline. The experiments were allowed to run several hours to determine if the particular velocity in use would destratify the model eventually. Runs at velocities associated with both Ri_1 and Ri_2 eventually mixed all but the bottom one-half inch of the model while the velocity associated with Ri_3

stabilized at two and one-half inches above the bottom. These comparisons indicate that the two highest velocities substantially penetrated the thermocline while the effectiveness of the velocity associated with Ri_3 would still be questionable. All three velocities were again tested with the contour in place and those results are discussed in a later section.

Another interesting observation was made on the height which the lens assumed when it leveled out. As was pointed out earlier, three different velocities were used corresponding to each Richardson number. The higher the pump velocity, the deeper the lens leveled out below the surface. Only one-half inch difference existed between the depth the lens leveled out for the highest velocity and the depth the lens leveled out for the lowest velocity. This may seem an insignificant difference, but when it is considered that this difference is almost 50 percent of the thermocline thickness, it could indicate how effectively the jet has penetrated the thermocline. Further observations indicated that the deeper the lens leveled out, the closer the destratification process approached completion.

The lensing phenomenon was very clear in the photographs and the growth of the lens could be observed. The lens would invariably level out somewhere in the region of the thermocline for all three velocities used. The initial growth of the lens was upward until the lens had reached the sides of the tank. The thermocline formed a table or barrier on which the bottom of the lens rested. When the lens had reached the side of the tank, the lens would grow both upward and downward at about equal rates. When the lens had grown to a thickness of about six inches, leaving three inches of unmixed water on the bottom

and one and one-half inches of the top water unmixed, the lens would begin to grow only upward. When the lens had reached the surface of the model, it began to slowly grow towards the bottom. This sequence of growth would seem to indicate that the jet initially penetrates the thermocline and the top water mixes easily with the heavier solution of the thermocline. As the lens grows, the jet of top water penetrates the lens and mixing with the thermocline still occurs. When the lens has grown to a point where the momentum of the jet can no longer penetrate the entire thickness of the lens, the lens begins to grow only to the top. In this case, the top water is mixing only with the intermediate density fluid of the lens. When the intermediate density of the lens finally reaches the intake of the pump, the weight of the fluid in the lens, which is heavier than the original fluid at the intake, can again penetrate to the heavier water near the bottom. Depending on the initial velocity of the jet, the lens will now grow to some point near the bottom. The successful mixing of the model is an indication that turbulent mixing has occurred or that the jet is in the turbulent flow regime.

One of the most important decisions in designing the contour was what portion of the fingers, if any, could be ignored. The final decision was made on the basis of the previous results. When the lens finally reached the stage of upward growth only, the water the pump forced downward was drawn from the lighter top water. It was believed that the top water contained in the contours fingers would be drawn to the pump when the lens began growing upward. Any part of the fingers deleted in the construction of the contour would have resulted in a loss of top water which would have been drawn to the pump. Since the destratification process is the mixing of two volumes of water, it was

decided that any volume of top water left out due to the deletion of any section of the fingers might possibly cause considerable discrepancies in the final results, and all the fingers were therefore made part of the contour. It was left to the series of experiments with the contour in place to justify this decision.

Contour Results

The observations made in the previous section were also made during tests with the contour in place. Again the high salt concentration solutions made it extremely difficult to observe visually the penetration of the thermocline by the jet. The lensing phenomenon itself could again be seen very clearly and photographs of the lens from one test run are presented in Figure 15. In the second series of experiments the criterion for thermocline penetration was the ability of the particular velocity in use to destratify the model. The model was assumed to be destratified when the density profile became uniform between one-half inch below the surface and one-half inch above the bottom of the model. A profile was considered uniform when the specific gravity varied less than 0.0005 between the two points described above.

All three Richardson numbers were again tested with the contour in place. As before, the velocity associated with Ri_3 failed to mix the bottom three inches of fluid. Since the velocity associated with Ri_3 would not destratify the model, and the lake being modeled was destratified, Ri_3 was eliminated as a possible parameter which would produce the best similarity between the model and the lake.

The lens growth, as described in the previous section, occurred in the same manner. Density profiles taken at intervals during the tests

also verified the visual observations of the lens growth.

The theoretical development for the potential energy curves was presented in Chapter IV. More adequate data is necessary to determine if potential energy curves can be useful in the study of lake destratification. The potential energy curves and a discussion are presented in Appendix F.

Observations were made in order to decide if the volume of water in the fingers was important. The basis on which the decision to place the fingers in the contour was discussed in the previous section. The dyed salt lens penetrated into every finger for experiments conducted with Ri_1 and Ri_2 as the non-dimensional velocities. This is a clear indication that the volume of water in the fingers was drawn into the pump and mixed and that the fingers are an important part of the model and should not be left out. A series of photographs are presented in Figure 16 which show the progress of the dyed salt lens into the fingers.

An interesting trend was found while studying the density profiles recorded during the tests. The portion of the profiles taken through the lens in the model showed, in every case, a uniform density through the lens. This is not the case for the profiles taken from Hamm's lake. The Hamm's lake density profiles vary from a lighter to a heavier density through the lens during the entire destratification process. This trend is illustrated in the comparative profiles for the model and Hamm's lake in Figures 17-20. The variance of density through the lens of Hamm's lake can be attributed to some type of phenomena which was not or could not be simulated in the model.

The order of magnitude difference between the model's Reynolds number and the lake's Reynolds number, both based on depth, would

produce some difference in the mixing characteristics of each flow. More mixing of the lens with the surrounding fluid in the real lake might produce the difference in the density profiles recorded for the model and Hamm's lake. The vertical scale exaggeration could have elongated the density profile in the model to produce a more uniform profile through the lens. Wind blowing over the surface of the lake could cause some mixing and thus distort the profile of the lens, or the alternating cooling of the lake at night and heating in the day might cause changes in the profile of the lens. The cooling of the surface by rain and the eventual run-off into the lake also might cause distortion of the lens profile. Rather than attributing the difference in the models and Hamm's lake density profiles through the lens to a single cause, it is probable that a combination of factors caused the discrepancies.

As was discussed in the development of the three forms of Richardson number, each measured velocity can be non-dimensionalized to produce each type of Richardson number. Through Richardson number matching, as was done in the rectangular tank and is illustrated in Table I of Appendix E, three velocities were obtained. A velocity, u_1, was used to form the Richardson number, Ri_1, and another velocity, u_2, was used to form the Richardson number, Ri_2, etc. By this process, three primary Richardson numbers, Ri_{11}, Ri_{22}, and Ri_{33}, were obtained and three separate experiments were conducted with the above parameters. Each velocity could additionally be non-dimensionalized to produce the other types of Richardson numbers, i.e., u_1 was used to form the Richardson number Ri_2. For the three initial velocities, nine non-dimensional velocities were calculated. The results of the above procedure are

presented in Table II of Appendix E. The significance of this procedure is being able to apply the data obtained through one velocity to three non-dimensional parameters, each parameter having non-dimensionalized the same velocity.

The time required for each velocity to completely destratify the model was recorded. The time was then non-dimensionalized with t' to produce a value of τ, the non-dimensional time for complete destratification.

Each form of Richardson number, or non-dimensional velocity, can now be plotted against the non-dimensional time it required to destratify the lake. In the same way, the value of the non-dimensional velocity of Hamm's lake can be plotted as a function of τ on the same plots as the non-dimensional model parameters. In this way the pair of non-dimensional parameters, a Richardson number and the non-dimensional time, which best match can be found. The results are presented in Figures 21, 22, and 23. Uncertainty bands have been added to the figures with the use of the estimated errors calculated in the error analysis in Appendix G.

Considering the results illustrated in Figures 21, 22, and 23, the most appropriate non-dimensional parameter in modeling artificial lake destratification is Ri_1. The minimum velocity for which complete destratification will occur can be estimated from Figure 21. The value probably lies somewhere in the error band, producing a value somewhere between 0.044 ft/sec and 0.062 ft/sec.

The other method used to compare the results are the density profiles of the model and Hamm's lake. Density profiles were recorded at intervals during each experiment. The models density profiles were

reduced by equation (4-1) and the time at which they were recorded was non-dimensionalized to give a value of t*. The density profile from Hamm's lake, recorded at the same t*, and the reduced model profile were plotted on the same figure. The profiles recorded for the non-dimensional parameter Ri_1 are presented, for three non-dimensional times, in Figures 17, 18, and 19. Likewise, a profile for Ri_2 is presented in Figure 20. The profiles produced using Ri_1, Figures 17, 18, and 19, show some similarity. The primary difference appears in the profile through the lens. As has been discussed previously, the density through the lens from Hamm's lake varied while the density through the lens in the model remained constant. This discrepancy probably occurs due to several factors as discussed before. With the use of Ri_2 as the primary non-dimensional parameter, the model did not destratify in the same non-dimensional time as the real lake. For a value of t* of 0.85, which is two times the value of τ, the density profile of the model and the density profile of Hamm's lake are presented in Figure 20.

Another natural phenomena can be observed in the profiles illustrated in Figures 17-19. The surface density point of the model and Hamm's lake interchange their relative positions. The data available from Hamm's lake were sometimes recorded in the morning and sometimes in the evenings. The changes in the surface temperature of the lake cause the top density point to vary, depending on whether the data was recorded in the morning or evening.

CHAPTER VI

SUMMARY AND CONCLUSIONS

Summary

The objective of this study was to determine the validity of a modeling technique for artificial lake destratification. The technique involved the use of vertical scale exaggeration. Observations in both the rectangular tank and the tank with the contour in place were used.

The tests using the rectangular tank showed the intermediate lens and the growth of the lens could be determined from photographic data. The contour model tests were designed using the data collected in the rectangular tank.

The results obtained with the contour in place confirmed the observations and data taken in the rectangular tank. It was demonstrated that the water contained in the fingers of the lake was drawn to the pump and mixed with denser water.

Density profiles taken from the model were compared to the profiles taken from Hamm's lake. The Richardson numbers, in conjunction with a non-dimensional time scale, were analyzed to determine the pair of non-dimensional parameters which would best model the real lake.

Conclusions

The conclusions of this study may be stated as follows:

1. The penetration of the thermocline by a jet of epilimnic water results in mixing and the formation of a lens of intermediate density. The lens remains level and spreads rapidly throughout the lake model producing a uniform layer. The growth of the lens occurs in stages, first growing equally upward and downward. The lens then grows upward to the surface and then downward to the bottom.

2. A lake which has not established stratification may be kept mixed by use of velocities smaller than those needed to mix it when it becomes stratified. However, after stratification has been established, there is a minimum velocity for complete mixing. The value of this velocity in the model is between 0.042 feet per second and 0.062 feet per second, corresponding to Ri_1 values of 900 and 433 respectively.

3. Comparing the density profiles from both Hamm's lake and the model, Ri_1 is the best non-dimensional parameter to model artificial lake destratification when used with the non-dimensional time scale developed.

4. The difference in the density profiles through the lens can be partially attributed to distortion caused by the use of vertical scale exaggeration and the difference in the model's Reynolds number and the Hamm's lake Reynolds number.

5. When analyzing each pair of non-dimensional parameters, a Richardson number and the time scale, the pair which best matched the parameters from Hamm's lake included the use of Ri_1 as the non-dimensionalizing parameter for velocity.

BIBLIOGRAPHY

(1) Barr, D. I. H. "Densimetric Exchange Flow in Rectangular Channels." La Houille Blanche, Vol. 18 (1963), 739-756.

(2) Barr, D. I. H. "Densimetric Exchange Flow in Rectangular Channels." La Houille Blanche, Vol. 22, No. 6 (1967), 619-630.

(3) Barr, D. I. H., and A. M. H. Hassan. "Densimetric Exchange Flow in Rectangular Channels." La Houille Blanche, Vol. 18, No. 7 (1963), 757-766.

(4) Barr, D. I. H. and B. E. Shaikh. "Model Simulation of Surface Profiles in Tidal and Non-Tidal Watercourses." The Engineer (London), Vol. 222, Pt. 2 (1966), 625-633.

(5) Brorchardt, J. A. "Eutrophication--Causes and Effects." American Water Works Association Journal, Vol. 61, Pt. 1 (1969), 272-275.

(6) Churchill, M. A. "Effects of Storage Impoundments on Water Quality." ASCE Sanitary Engineering Divisions Journal, Vol. 83, SA-1 (1971), 245-273.

(7) Francis, J. R. D. "Scaling of River and Estuary Models." Engineering (London), Vol. 190 (1960), 329-331.

(8) Hogan, Wm. T., F. E. Reed, and A. W. Starbird. "Optimum Mechanical Aeration Systems for Rivers and Ponds." Massachusetts: Littleton Research and Engineering Corp. Water Pollution Control Research Series Report No. 16080-DOO, 1970.

(9) Hooper, F. F., R. C. Ball, and H. A. Tanner. "An Experimentation in Artificial Circulation of a Small Michigan Lake." Transactions of American Fisheries Society, Vol. 82 (1952), 222.

(10) Irwin, W. H., J. M. Symons, and G. G. Robeck. "Impoundment Destratification by Mechanical Pumping." Sanitary Engineering Division Journal ASCE, Vol. 92, SA-6 (1966), 21-40.

(11) Kittrel, F. W. "Thermal Stratification in Reservoirs." Symposium on Streamflow Regulation for Quality Control. New York: Robert A. Taft Sanitary Engineering Center, PHS Publication No. 999-WP-30, 1965, pp. 57-67.

(12) Knoppert, P. L., et al. "Destratification Experiments at Rotterdam." American Water Works Association Journal, Vol. 62, Pt. 2 (1970), 448-454.

(13) Kouba, G. E. "Similitude Investigation of Vertical Exaggeration in Stratified Lake Models." (unpub. Master's thesis, Oklahoma State University, 1974).

(14) Ligget, J. A., and K. L. Kwang. "Properties of Circulation in Stratified Lakes." ASCE Hydraulics Divisions Journal, Vol. 97, Pt. 1 (1971), 15-29.

(15) Love, S. K. "Relationship of Impoundments to Water Quality." American Water Works Association Journal, Vol. 53 (1961), 559.

(16) Olds, F. C. "Scale Models Solve Water Flow Problems." Power Engineering, Vol. 74 (1970), 40-43.

(17) Parsons, R. M. "Temperature Prediction in Stratified Water: Mathematical Model-Users Manual." Massachusetts: Massachusetts Institute of Technology. Water Pollution Control Research Series, United States Environment Projection Agency, Report No. 16130-DJH, 1971.

(18) Policastro, A. J. and J. V. Tokar. "Heated-Effluent Dispersion in Large Lakes: State-of-the-Art of Analytical Modeling." Maine: Argonne National Laboratory, 1972.

(19) Prandtl, L. The Essentials of Fluid Dynamics. London: Blackie, 1952.

(20) Quintero, J. E. and J. E. Garton. "A Low Energy Lake Destratifier." Michigan: American Society of Agricultural Engineers. Paper No. 72-599, 1972.

(21) Robinson, E. L., W. H. Irwin, and J. M. Symons. "Influence of Artificial Destratification on Plankton Populations in Impoundments." Transactions of the Kentucky Academy of Science, Vol. 30 (1969), 71-104.

(22) Symons, J. M., J. R. Carswell, and G. G. Robeck. "Mixing of Water Supply Reservoirs for Quality Control." American Water Works Association, Vol. 62, Pt. 1 (1970), 322-334.

(23) Symons, J. M., W. H. Irwin, and G. G. Robeck. "Impoundment Water Quality Changes Caused by Mixing." ASCE Sanitary Engineering Division Journal, Vol. 93, SH-2 (1967), 1-20.

(24) Symons, J. M. et al. "Impoundment Destratification for Raw Water Quality Control Using Either Mechanical or Diffused Air Pumping." American Water Works Association Journal, Vol. 59, Pt. 2 (1967), 1268-1291.

(25) Teerink, J. R. and C. V. Martin. "Artificial Destratification in Reservoirs of the California State Water Project." American Water Works Association Journal, Vol. 61, Pt. 1 (1969), 272-275.

(26) Vogel, S. J. "Similitude Investigation of Vertical Exaggeration in Stratified Lake Models." (unpub. Master's thesis, Oklahoma State University, 1972).

(27) Woodward, R. L. and M. LeBosquet. "Effects of Reservoir Operation on Stream Water Quality." Public Health Reports, Vol. 64 (1949), 1223.

(28) Committee Report. "Artificial Destratification in Reservoirs." American Water Works Association Journal, Vol. 53, Pt. 2 (1971), 597-604.

(29) Task Group Report. "Chemistry of Nitrogen and Phosphorous." American Water Works Association Journal, Vol. 62 (1970), 127.

(30) Task Group Report. "Sources of Nitrogen and Phosphorous." American Water Works Association Journal, Vol. 59 (1967), 344.

(31) Task Group Report. "Nutrient Associated Problems in Water Quality and Treatment." American Water Works Association Journal, Vol. 58 (1966), 1337.

APPENDIX A

FIGURES AND ILLUSTRATIONS

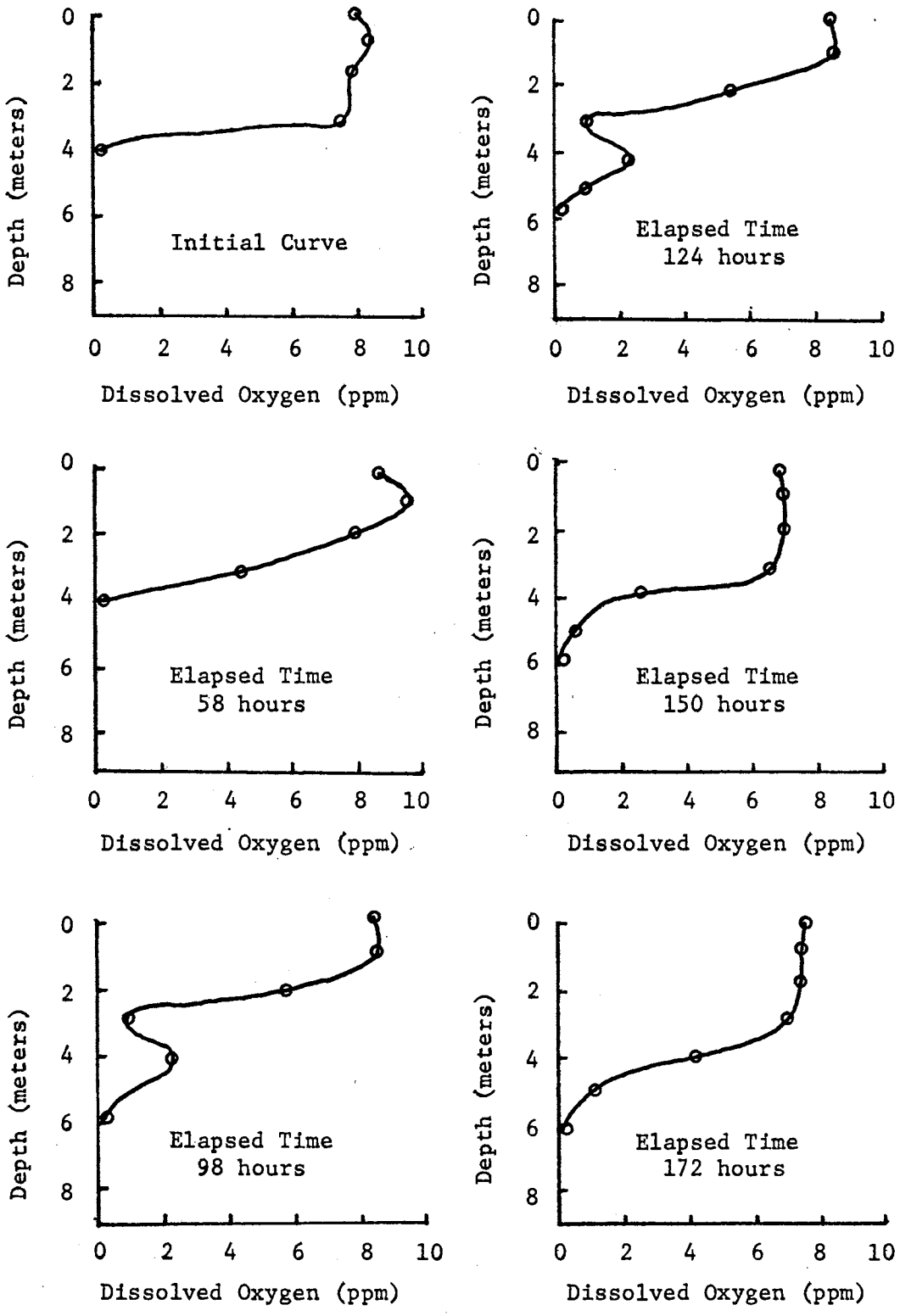

Figure 1. Dissolved Oxygen Profile Curves As A Function of Destratification Time

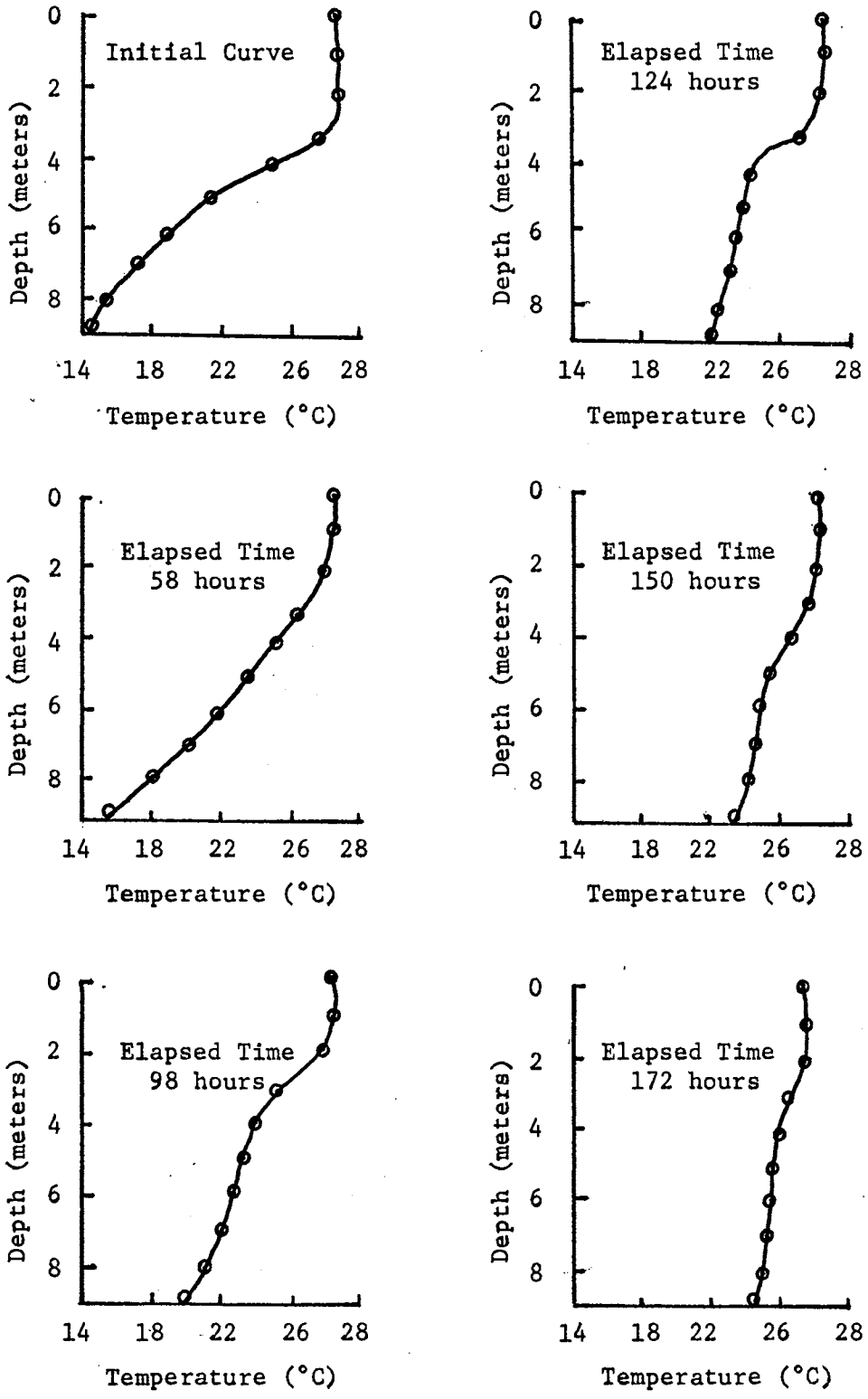

Figure 2. Temperature Profile Curves As A Function of Destratification Time

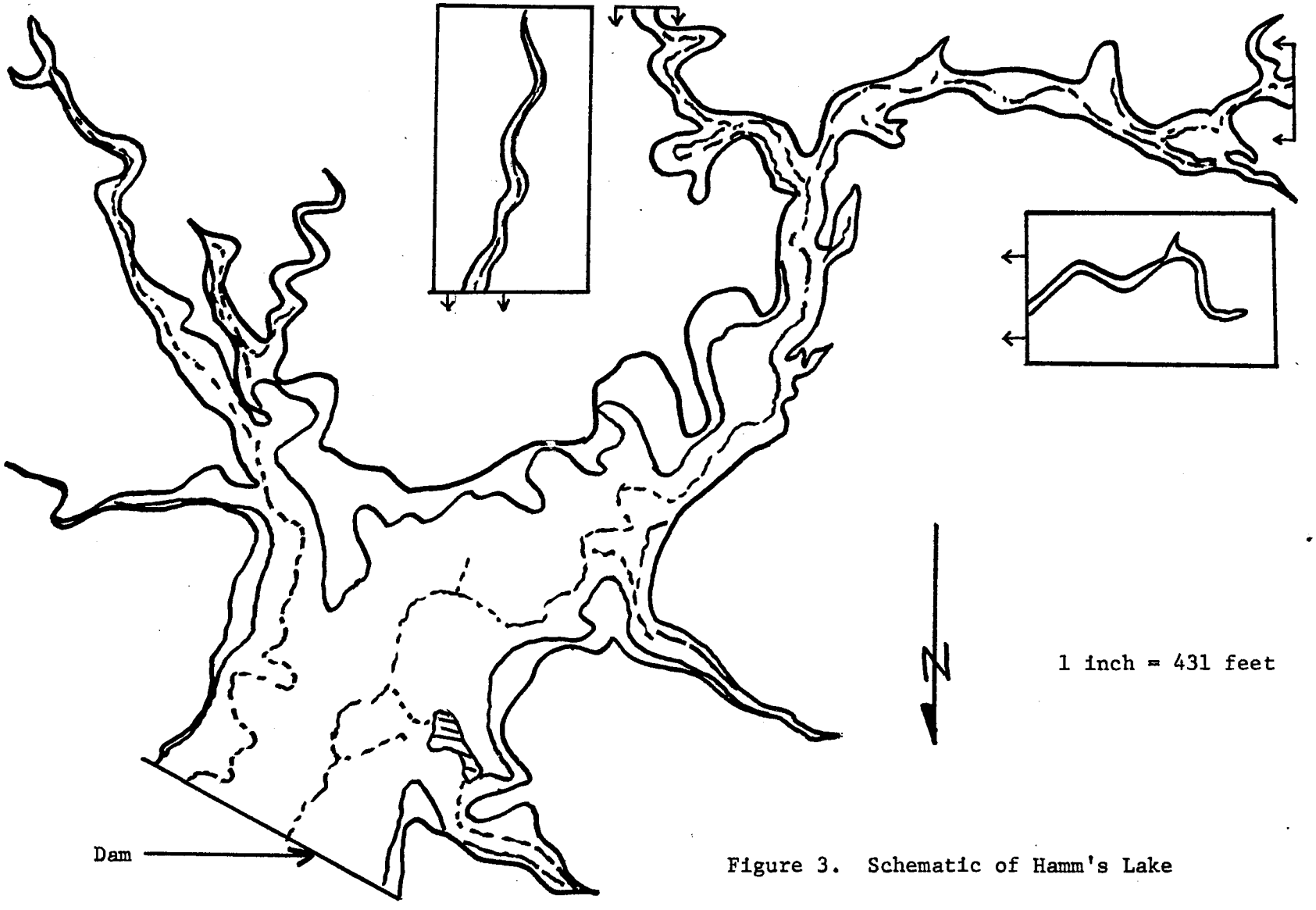

Figure 3. Schematic of Hamm's Lake

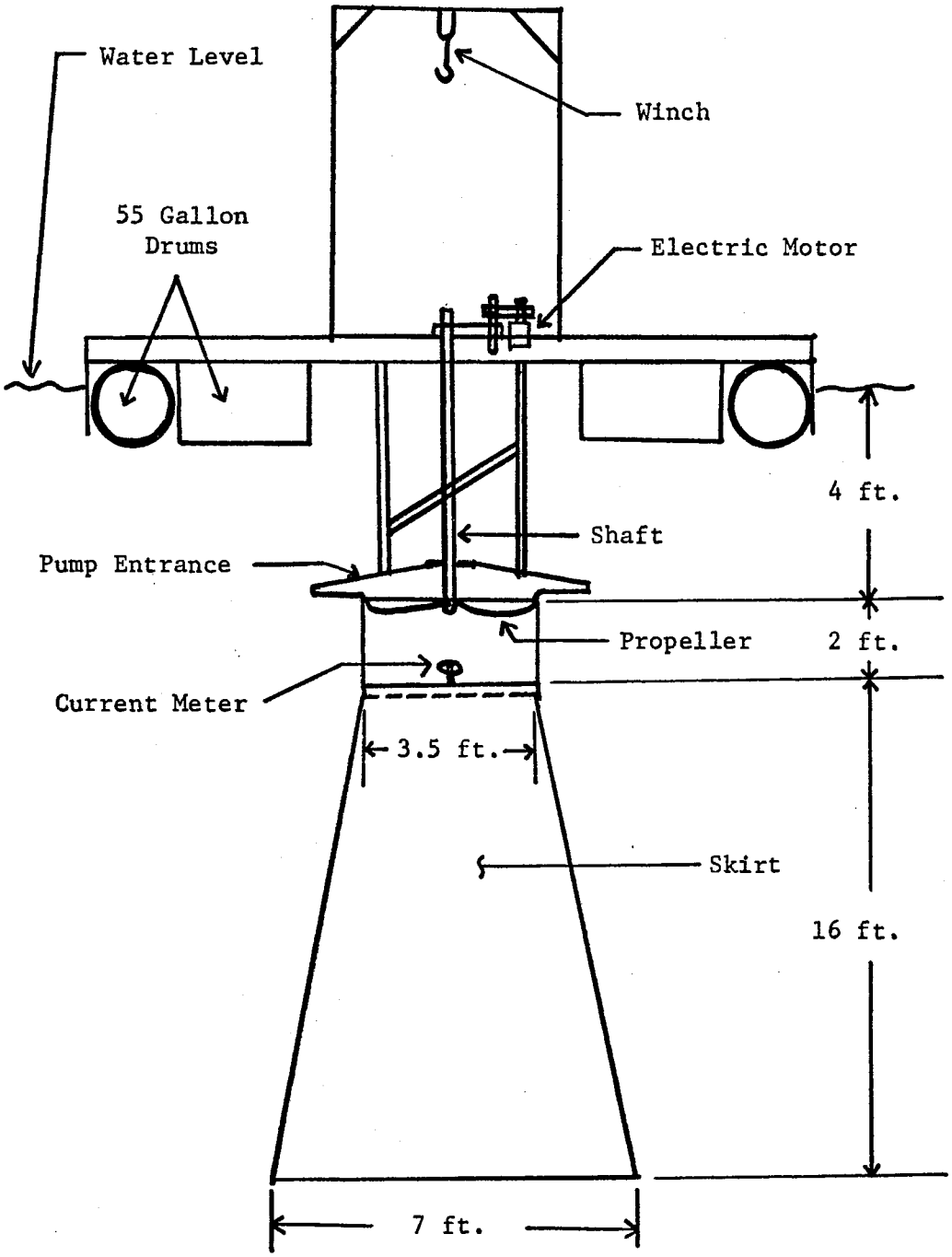

Figure 4. Schematic of Hamm's Lake Pump

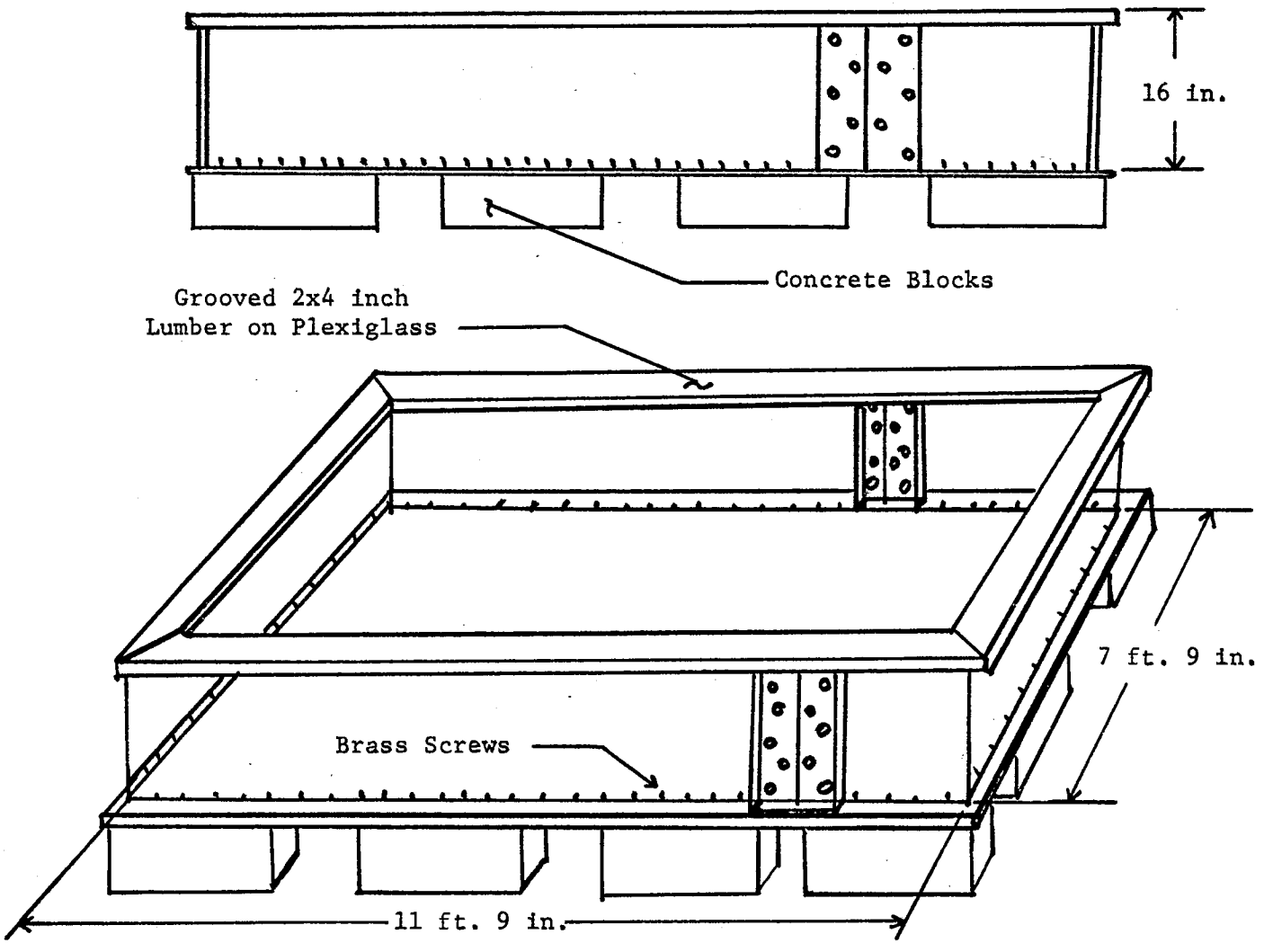

Figure 5. Schematic of Lake Model

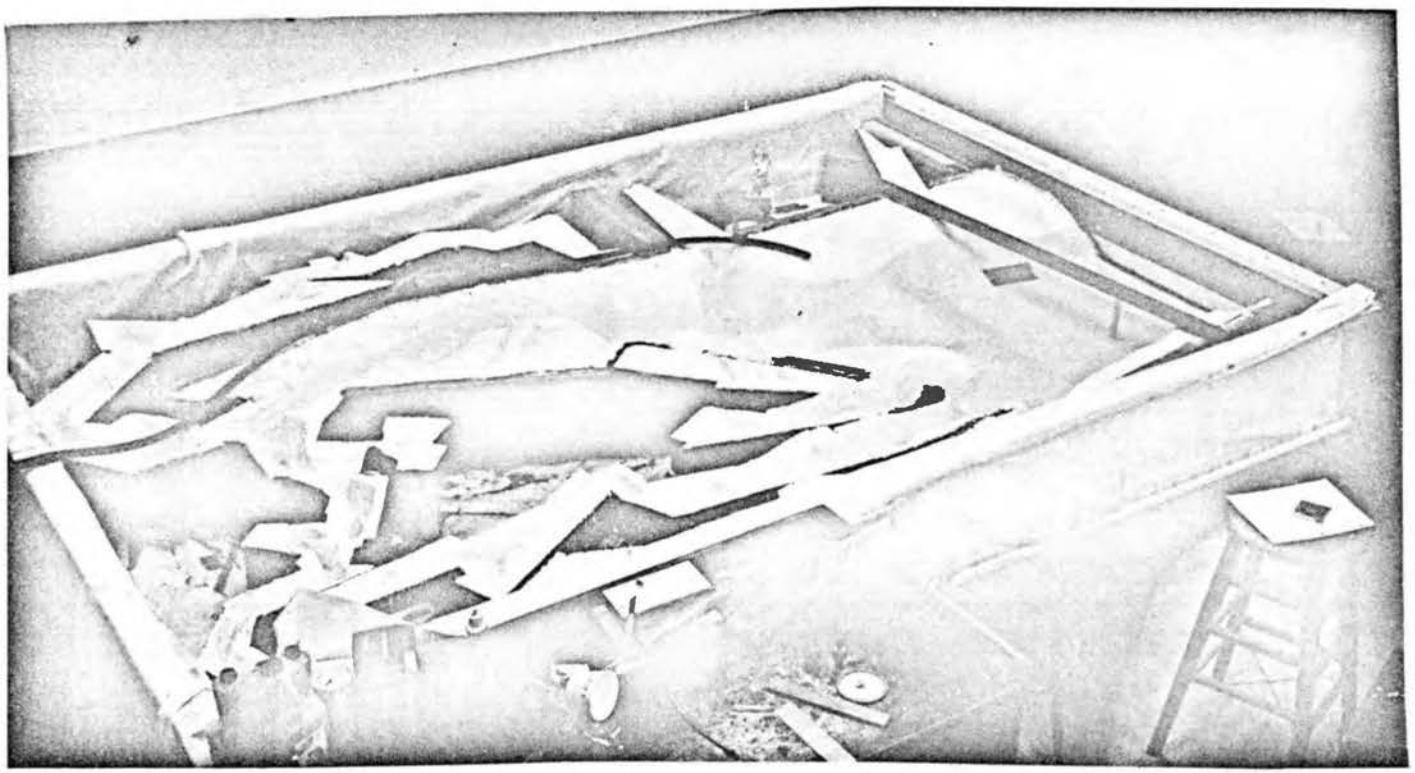

Figure 6. Photograph of Completed Contour

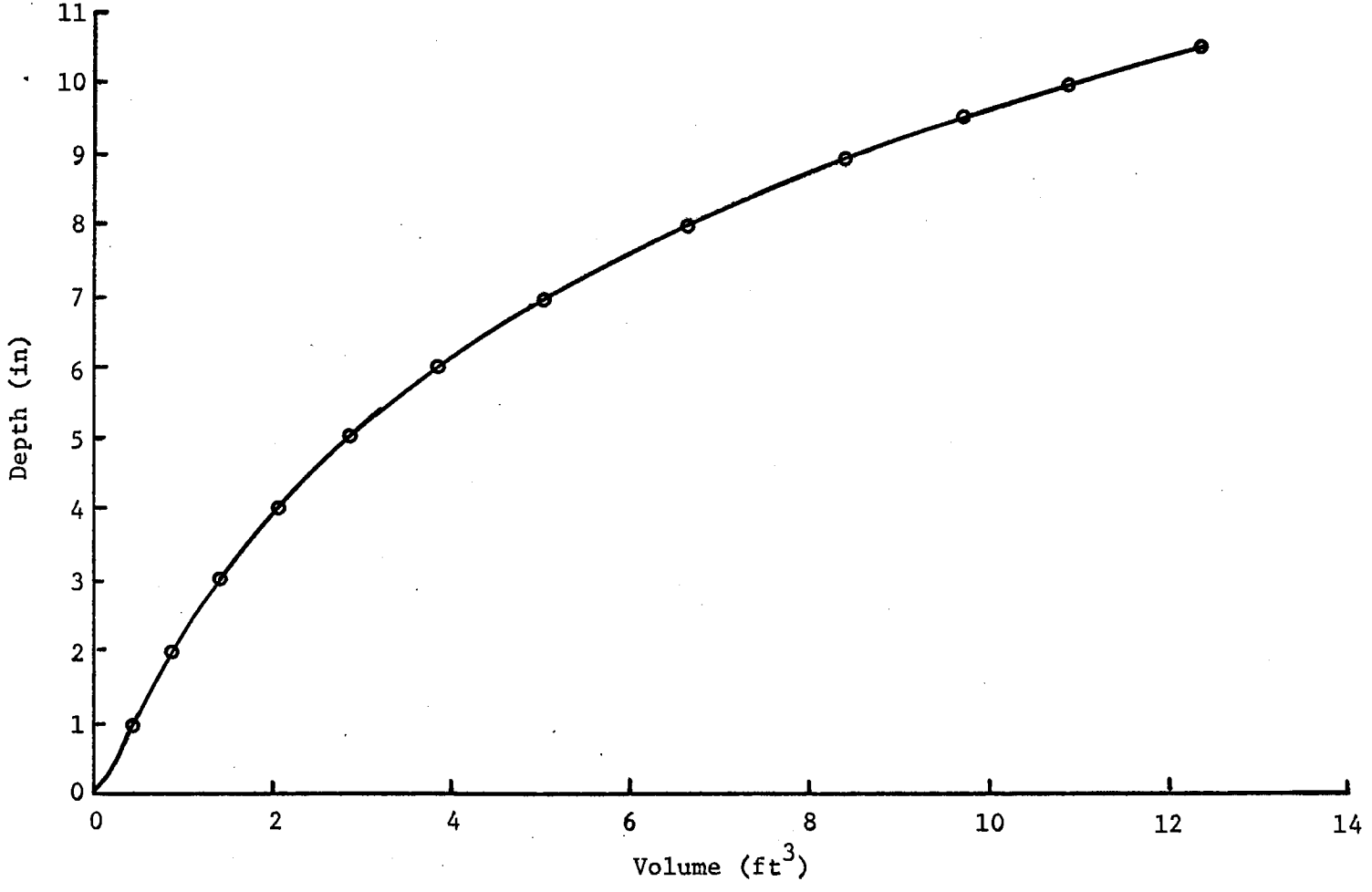

Figure 7. Fluid Volume of Model With Contour as a Function of Depth

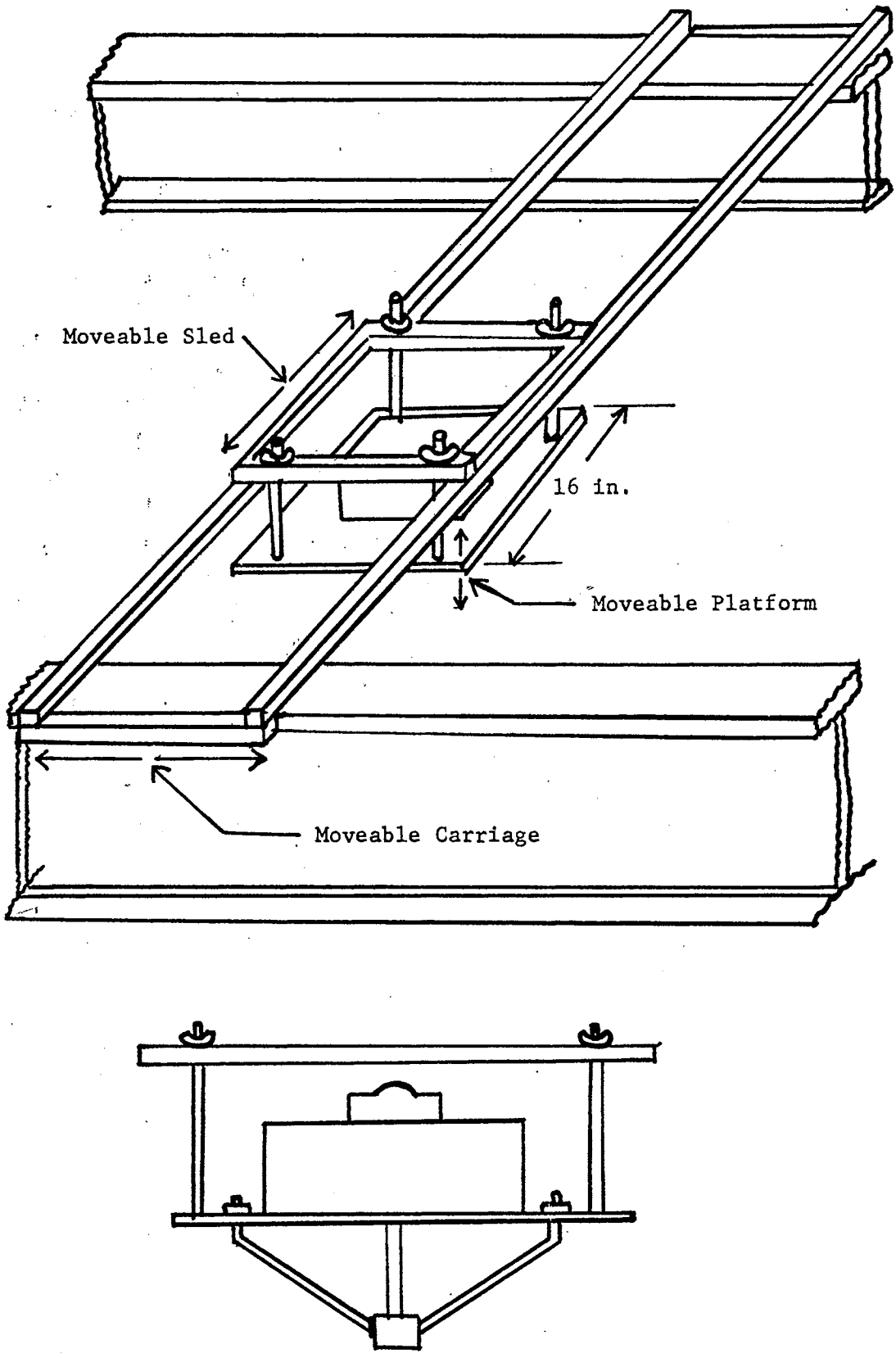

Figure 8. Pump Sled and Carriage

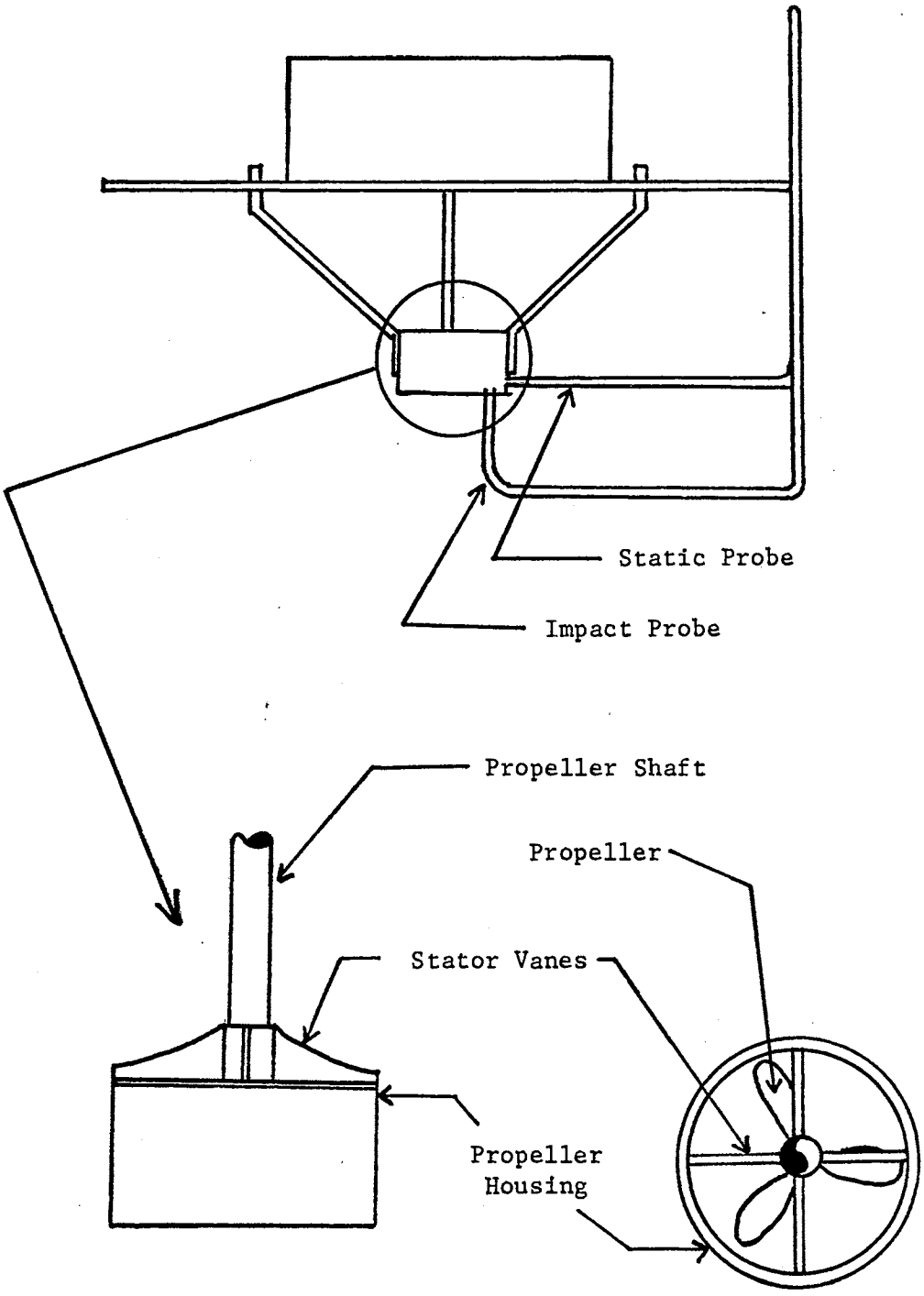

Figure 9. Manometer Attachment and Propeller Housing Details

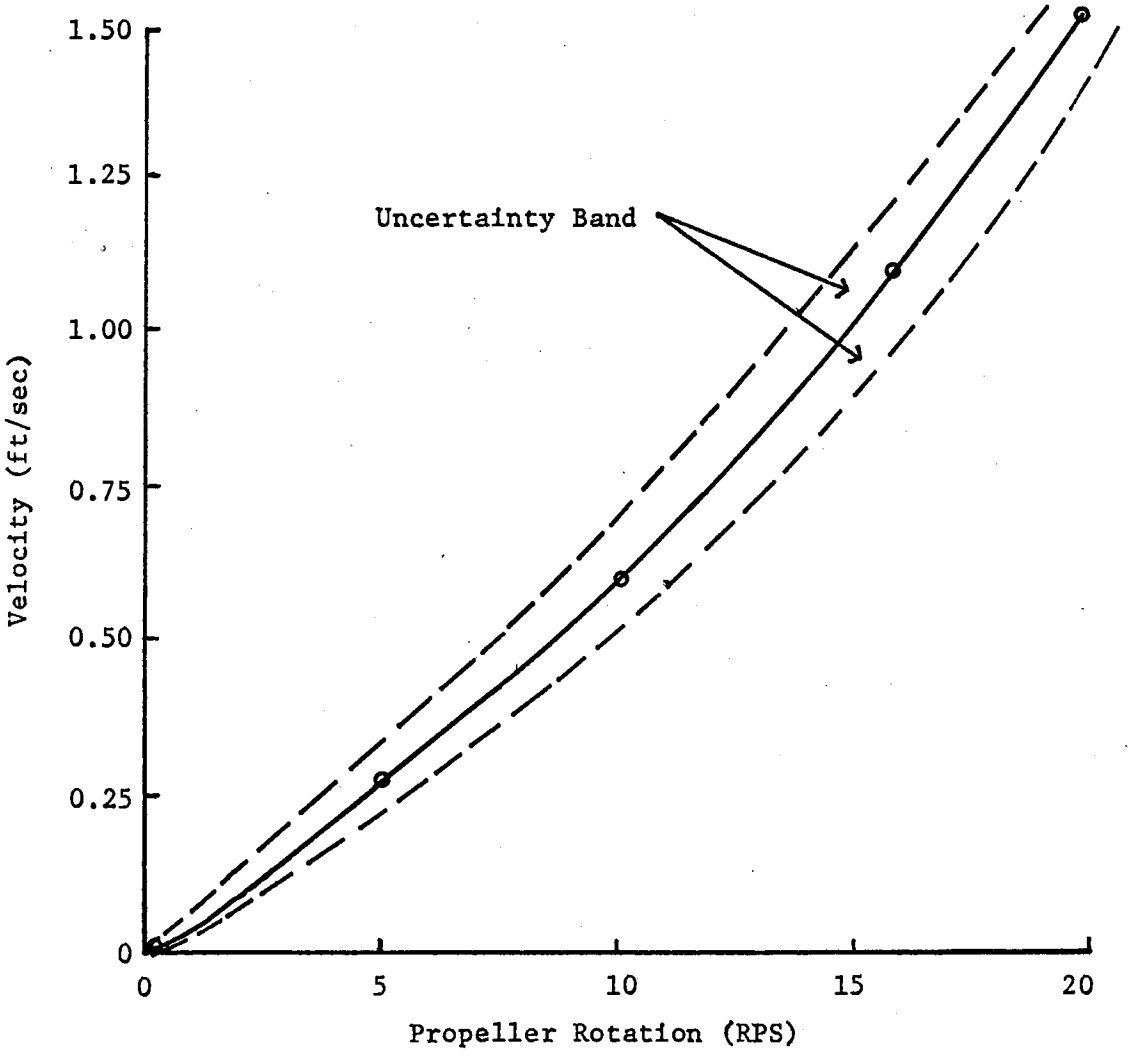

Figure 10. Velocity Calibration Curve for Known Shaft Rotation

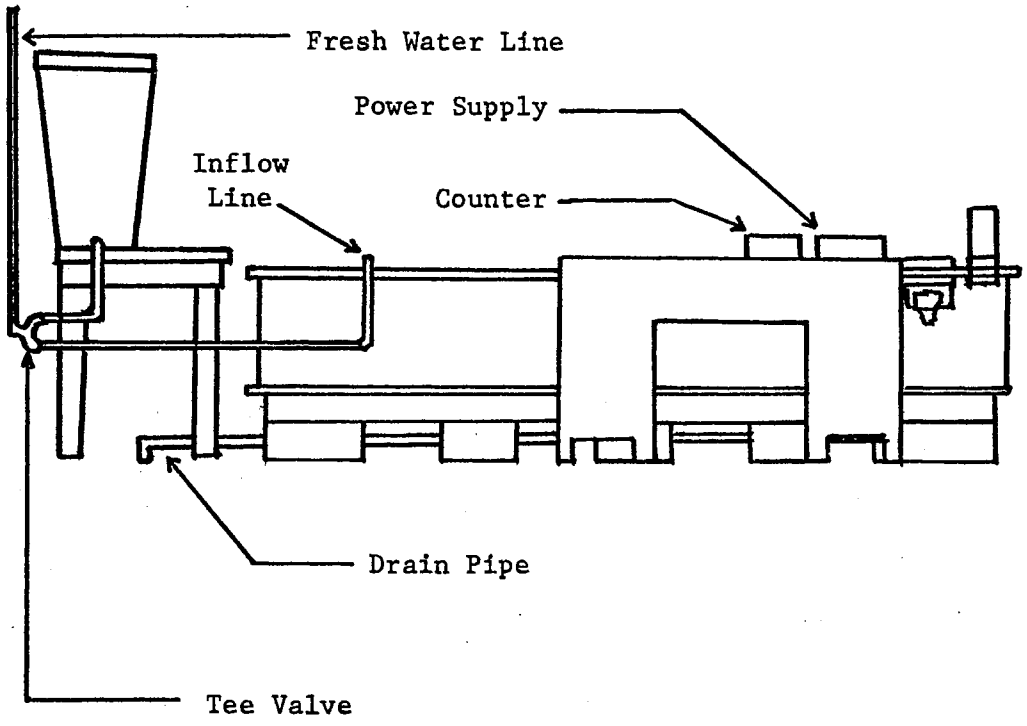

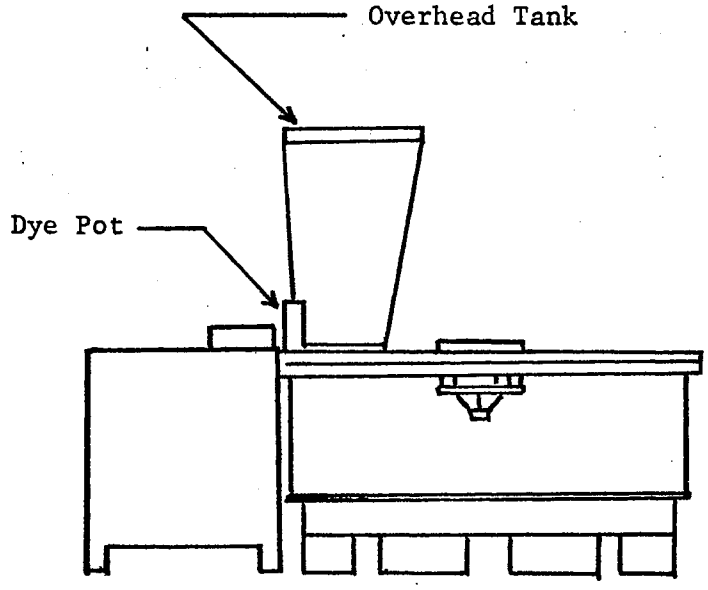

Figure 11. Schematic of Laboratory Facility

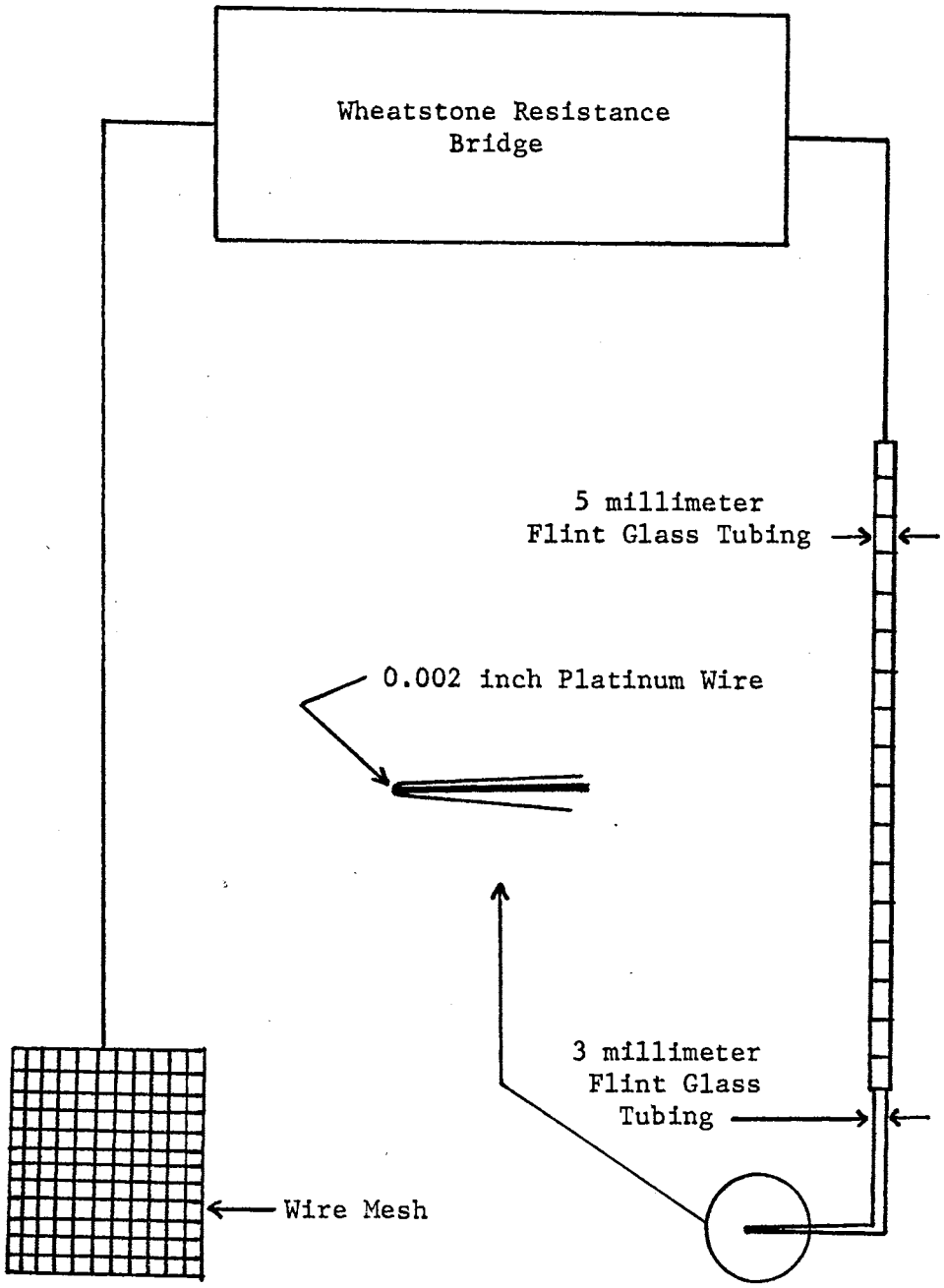

Figure 12. Conductivity Probe Details

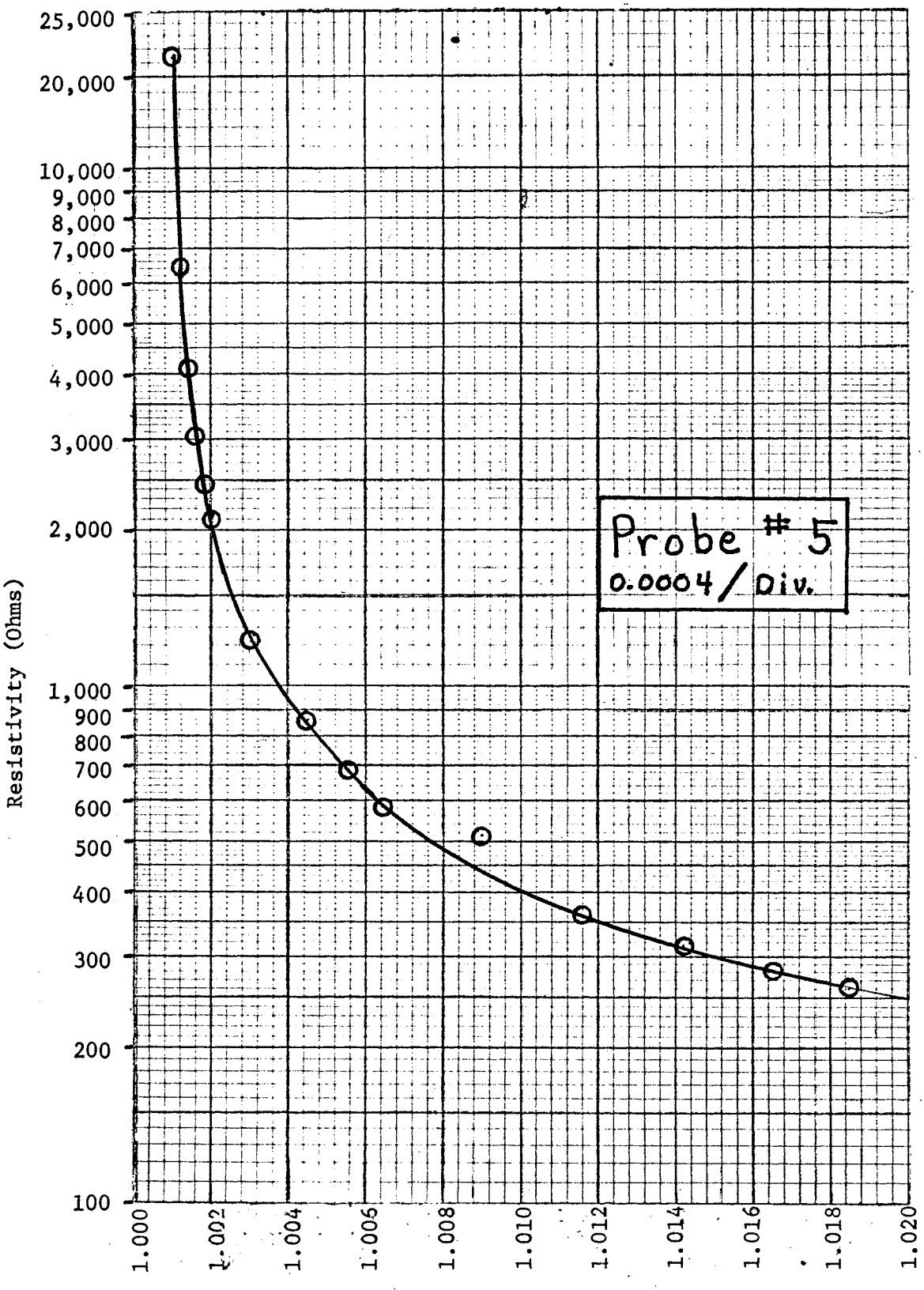

Figure 13. Conductivity Probe Calibration Curve

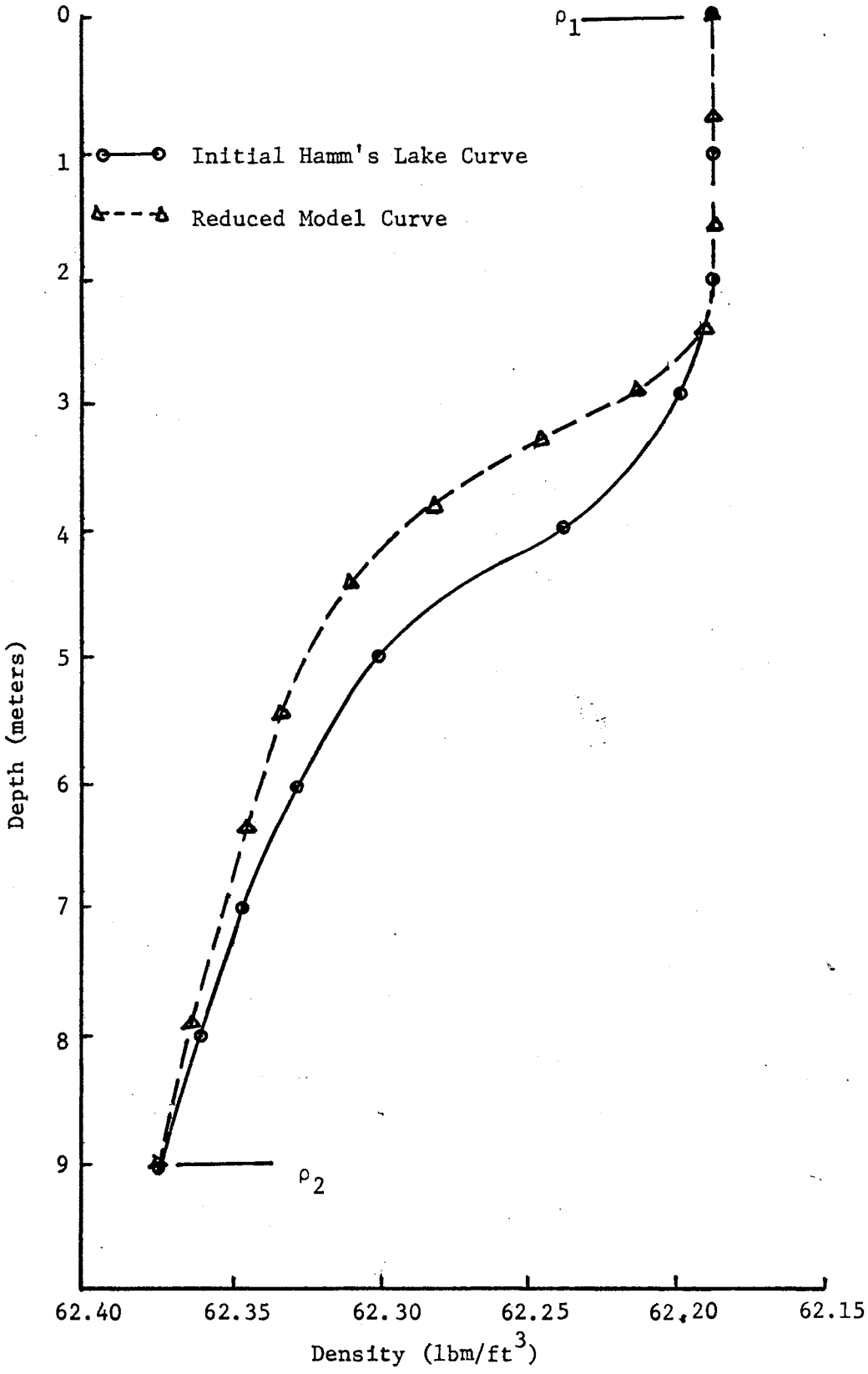

Figure 14. Comparison of Initial Hamm's Lake Curve and Initial Model Curve

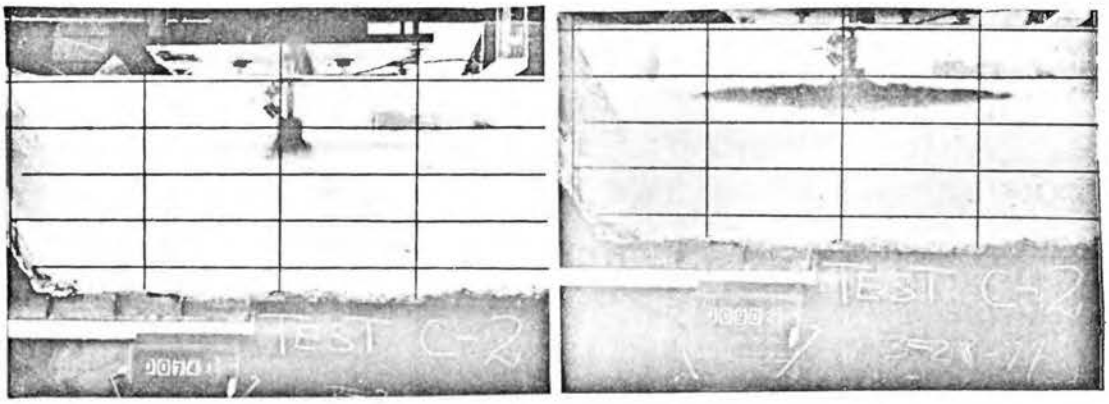

Elapsed Time 3 Seconds

Elapsed Time 18 Seconds

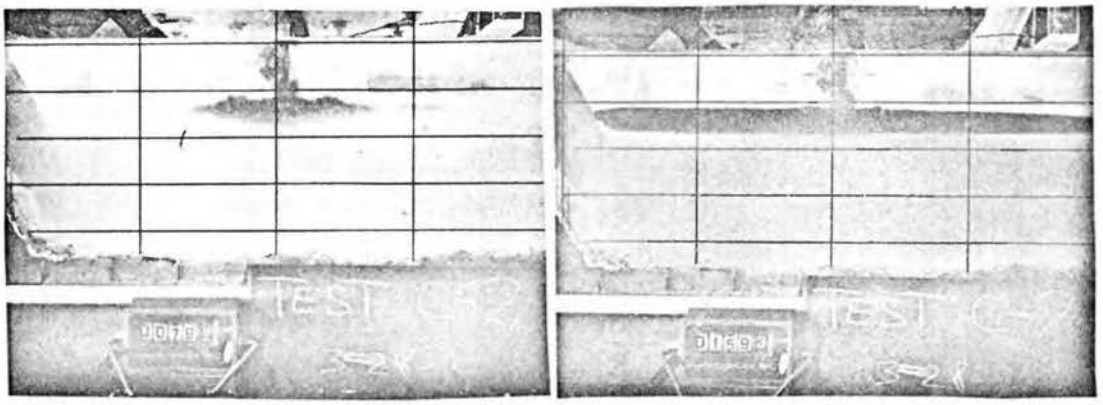

Elapsed Time 8 Seconds

Elapsed Time 88 Seconds

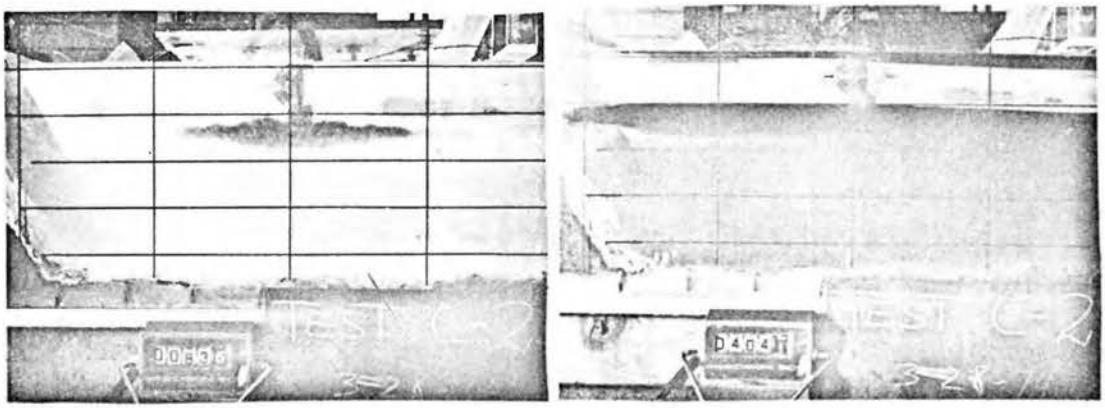

Elapsed Time 12 Seconds

Elapsed Time 333 Seconds

Figure 15. Visualization of the Lensing Phenomenon for u=0.1615 ft/sec

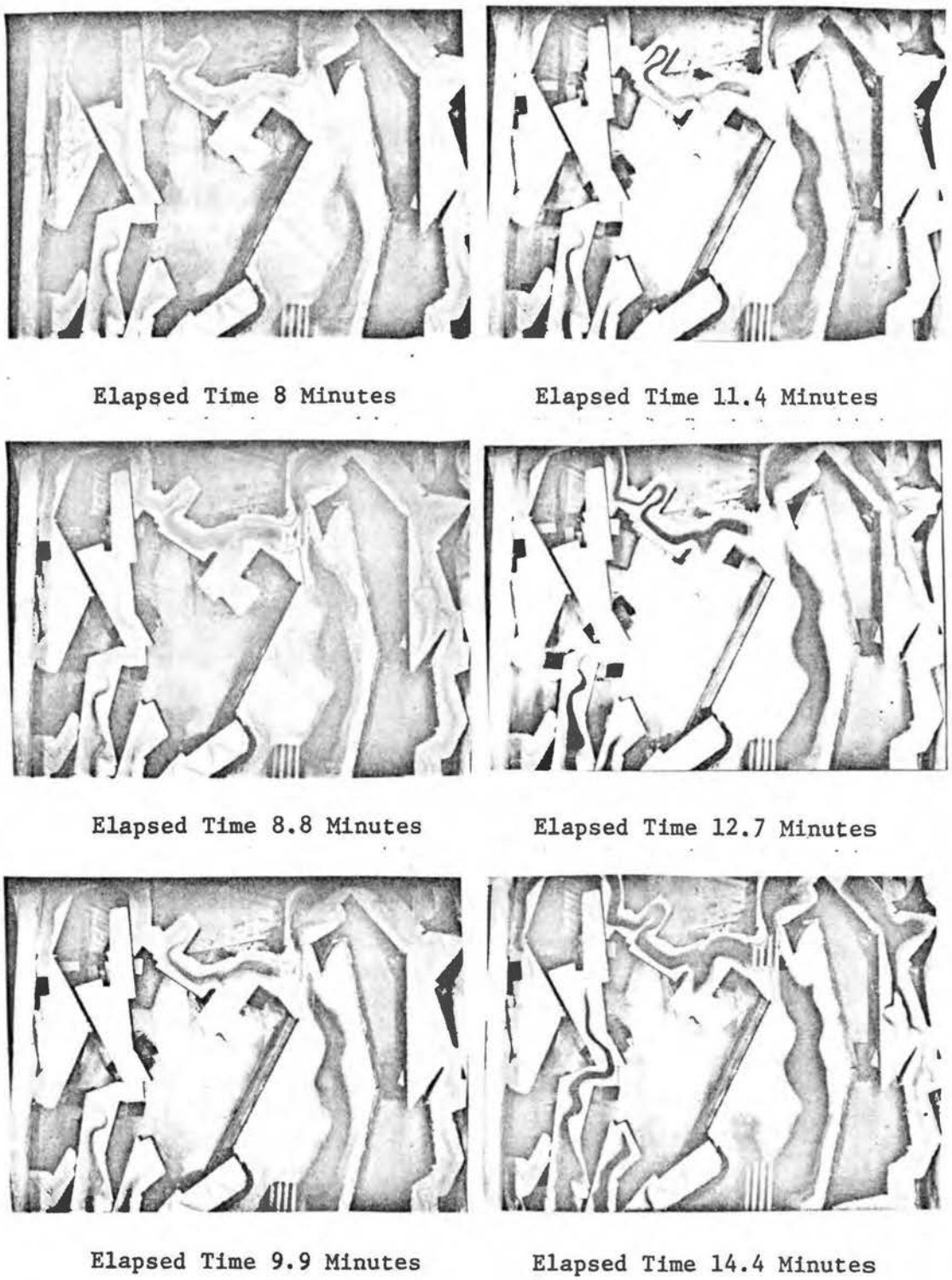

Elapsed Time 8 Minutes

Elapsed Time 11.4 Minutes

Elapsed Time 8.8 Minutes

Elapsed Time 12.7 Minutes

Elapsed Time 9.9 Minutes

Elapsed Time 14.4 Minutes

Figure 16. Lens Penetration of the Fingers for u=1.053 ft/sec

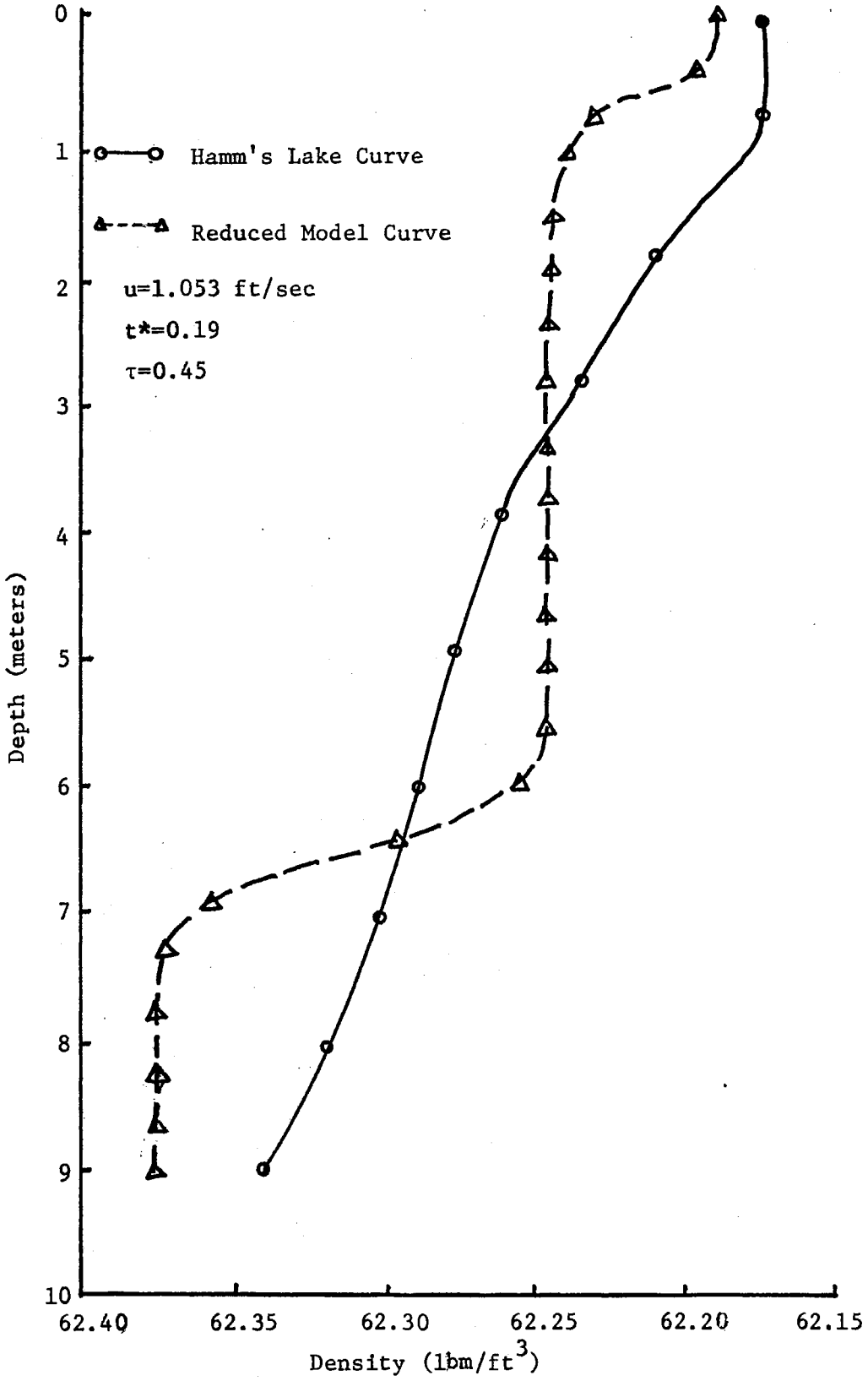

Figure 17. Comparison of Hamm's Lake Curve and Model Curve For Ri_1

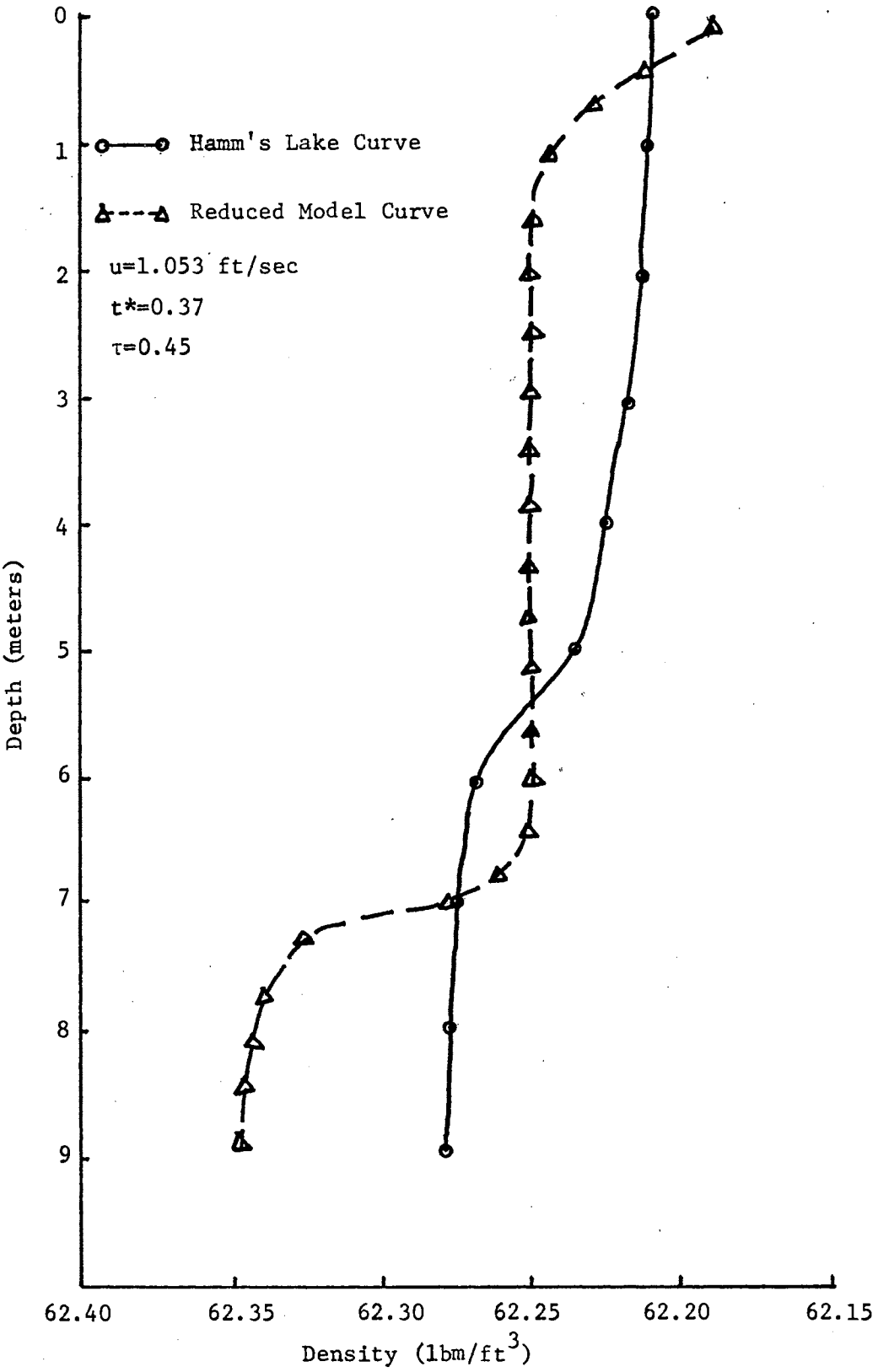

Figure 18. Comparison of Hamm's Lake Curve and Model Curve for Ri_1

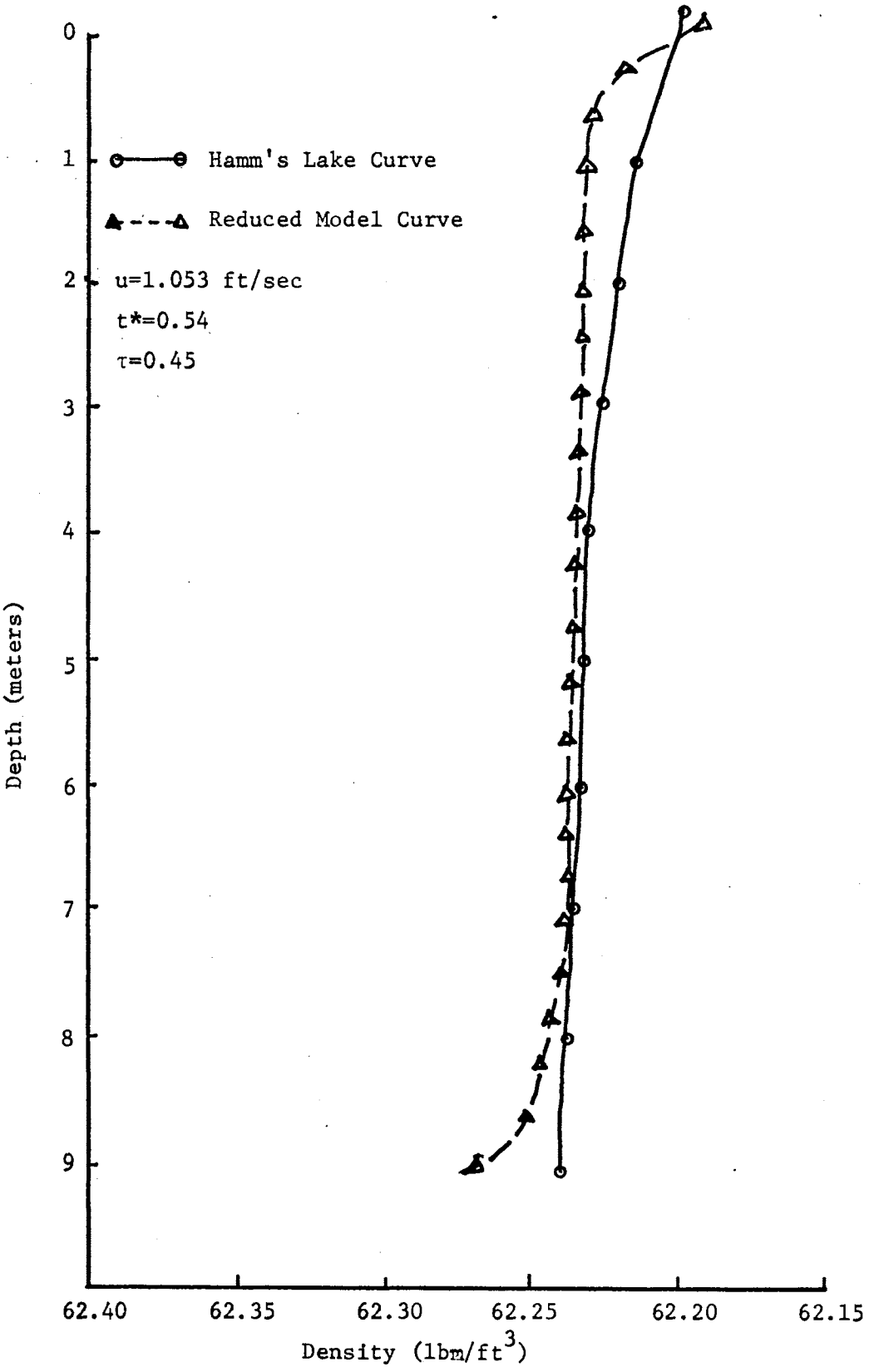

Figure 19. Comparison of Hamm's Lake Curve and Model Curve for Ri_1

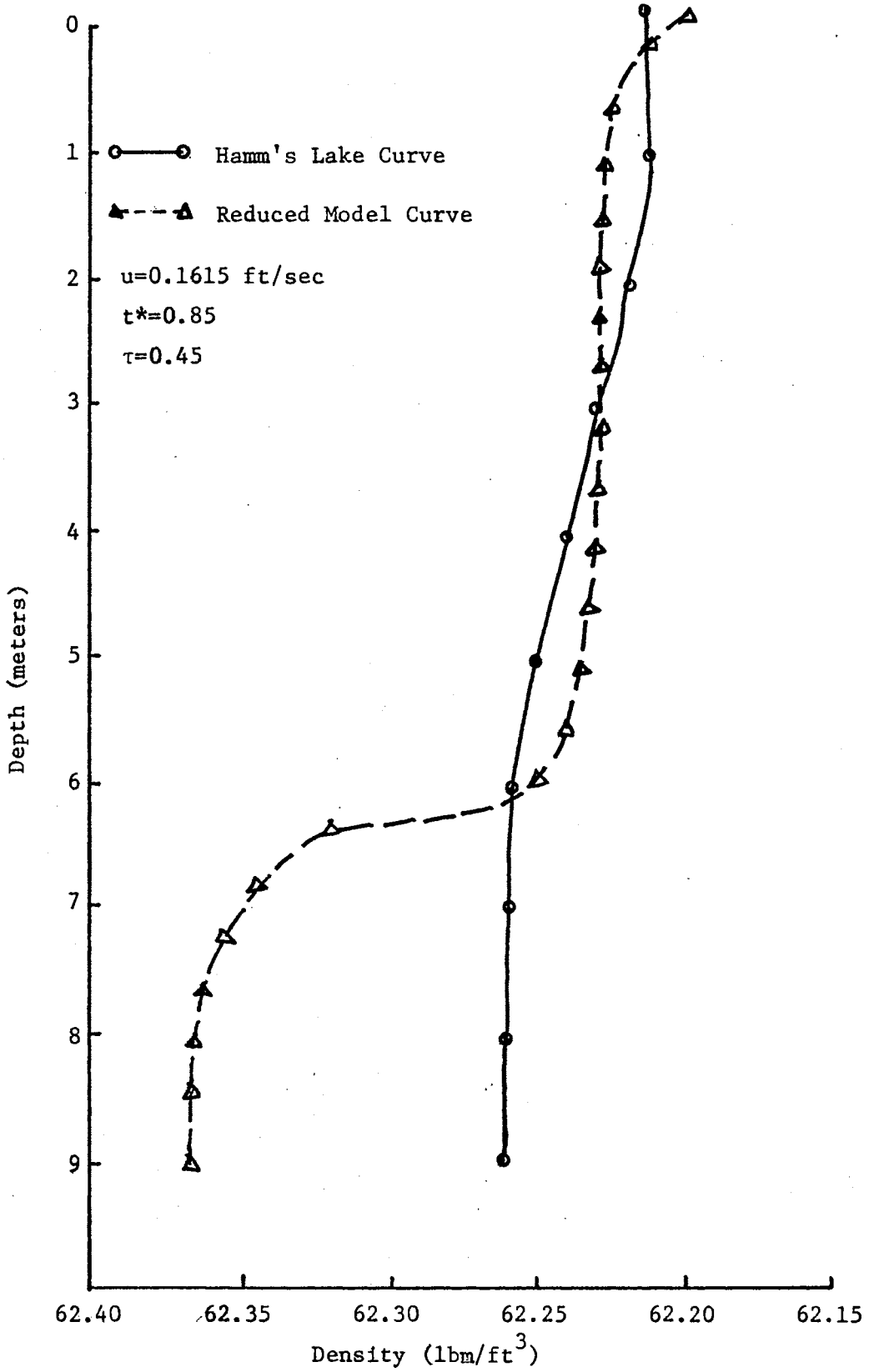

Figure 20. Comparison of Hamm's Lake Curve and Model Curve for Ri_2

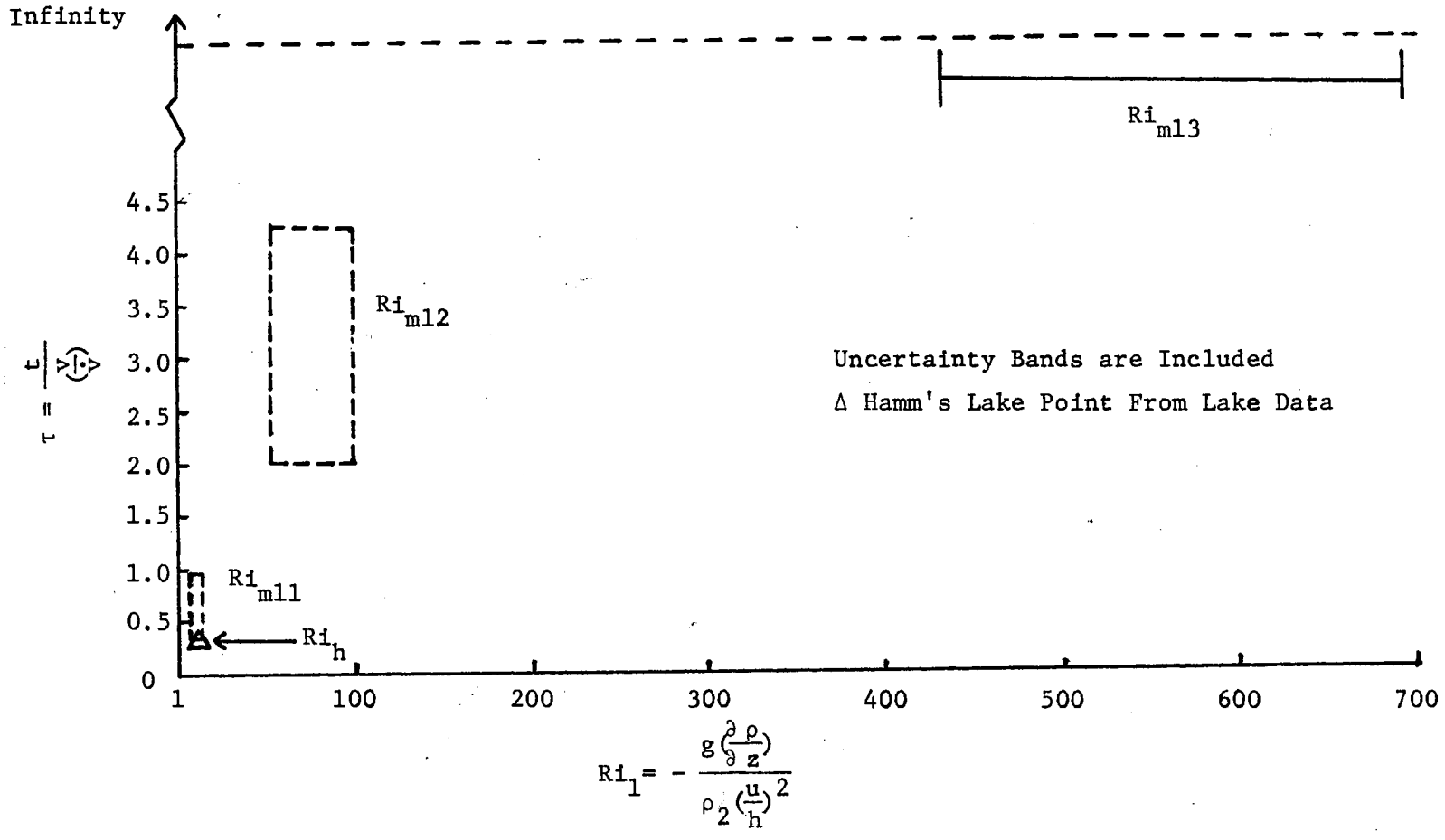

Figure 21. Non-dimensional Time as a Function of Richardson Number 1 or Non-dimensional Velocity

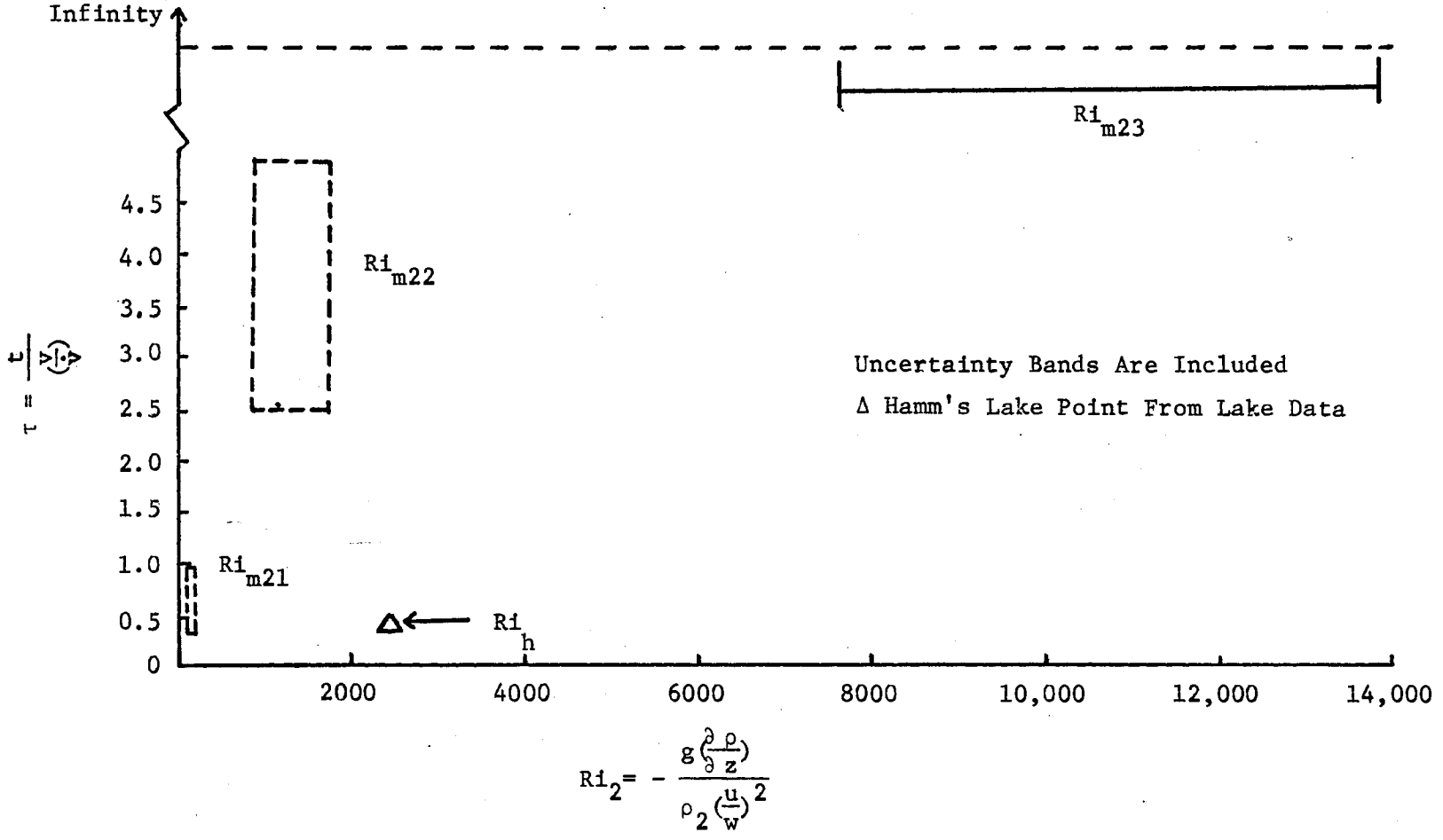

Figure 22. Non-dimensional Time as a Function of Richardson Number 2 or Non-dimensional Velocity

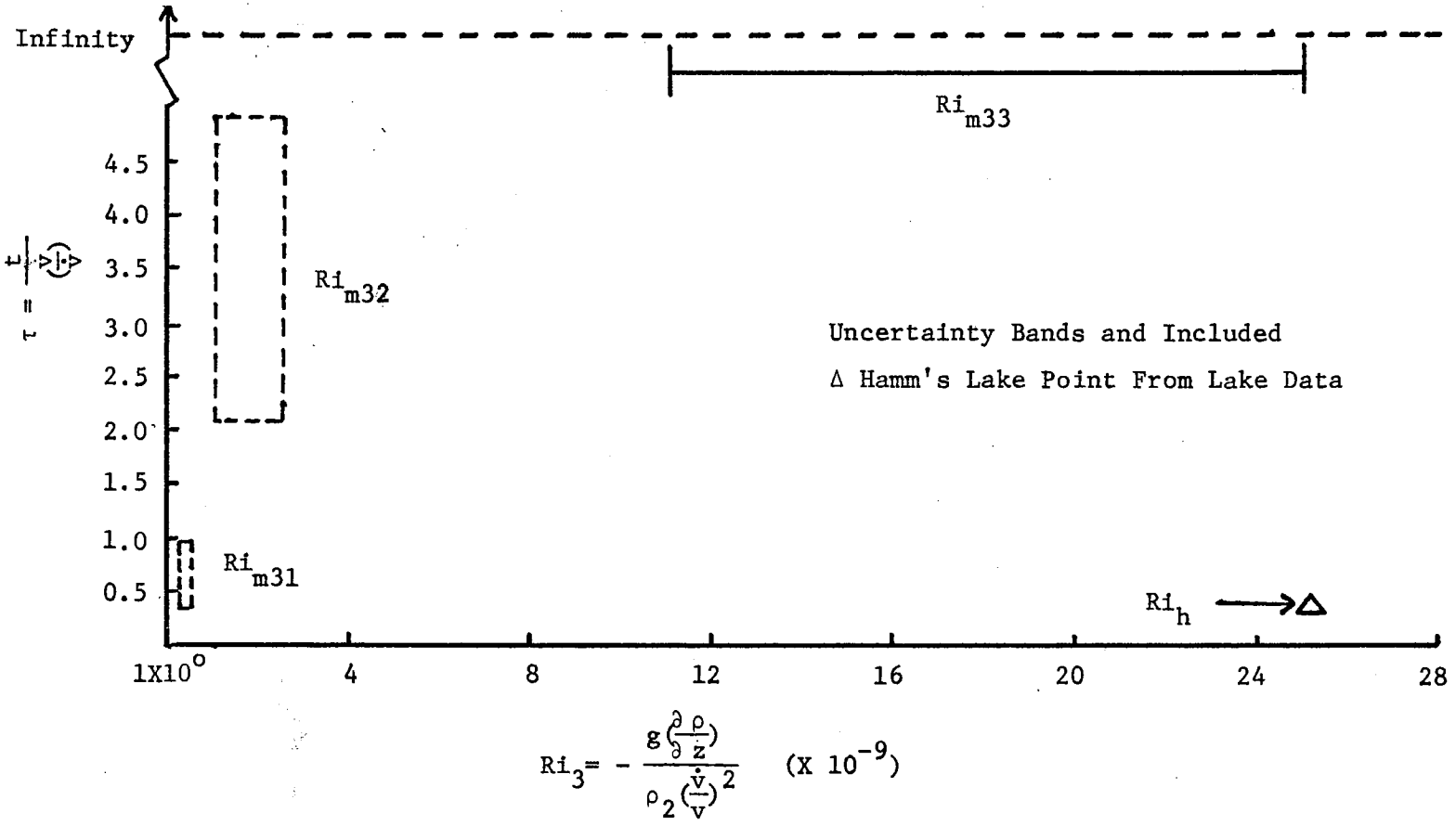

Figure 23. Non-dimensional Time as a Function of Richardson Number 3 or Non-dimensional Velocity

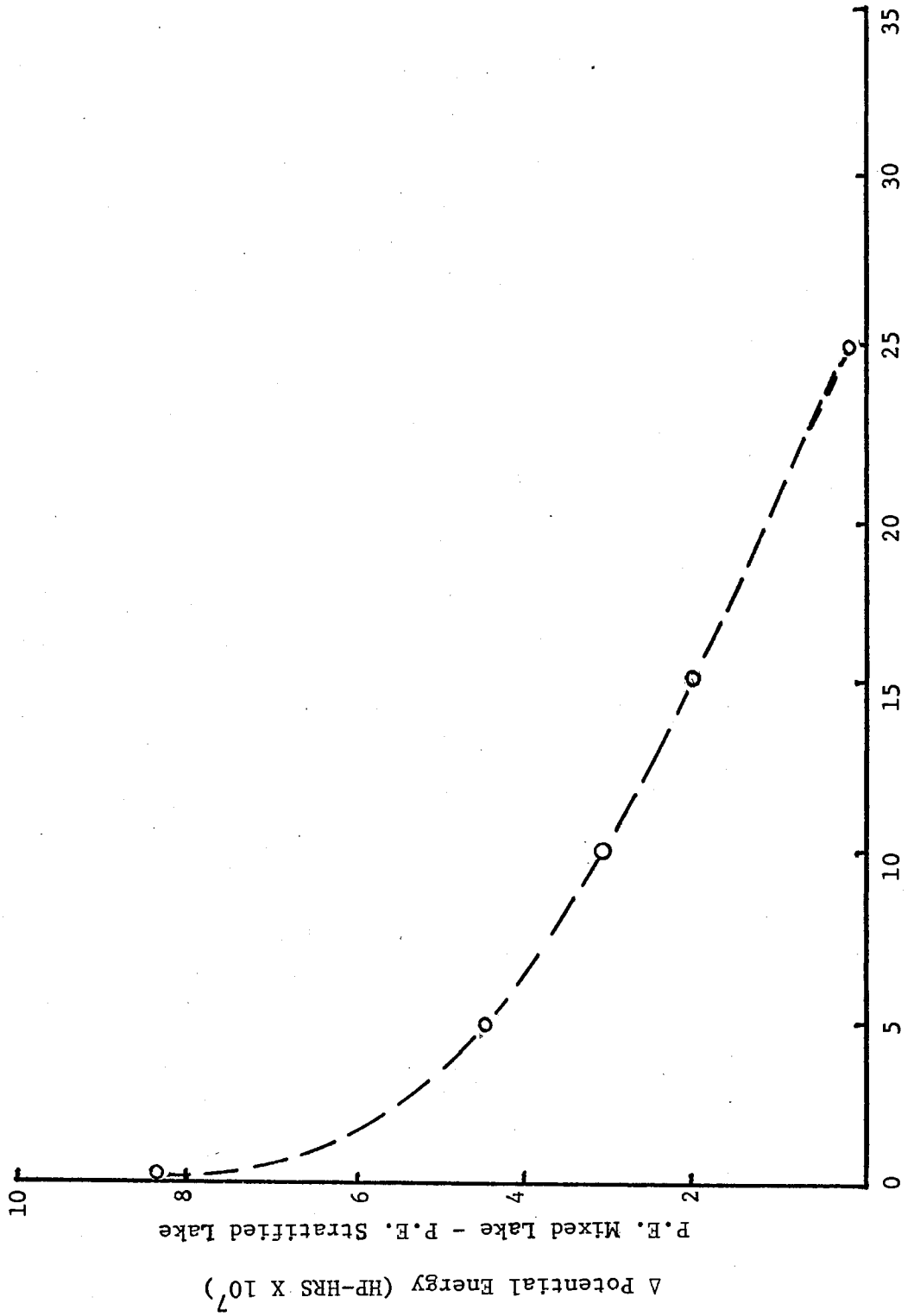

Figure 24. Model Potential Energy Curve

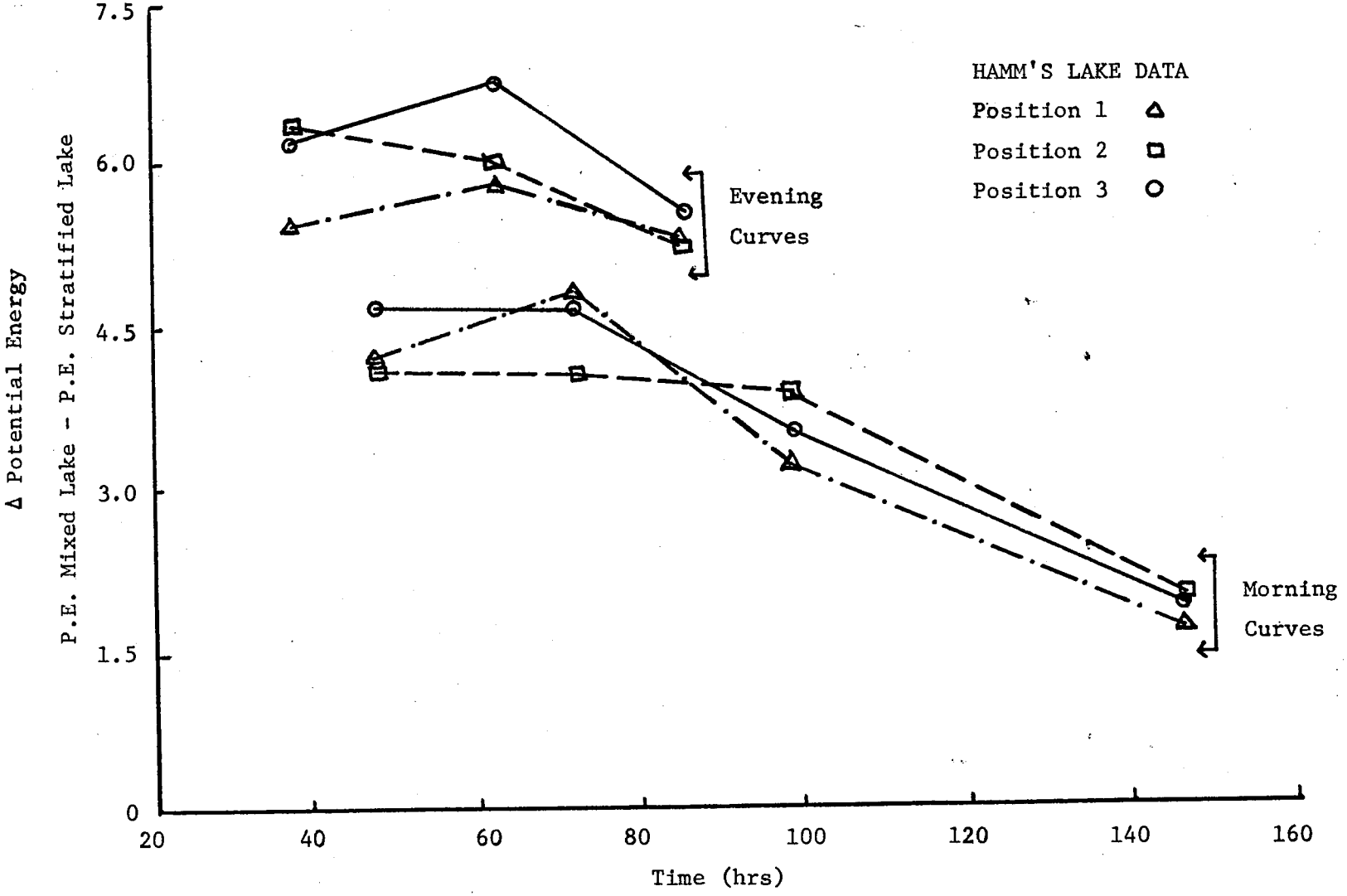

Figure 25.. Hamm's Lake Potential Energy Curve

APPENDIX B

VELOCITY CALCULATION

APPENDIX B

VELOCITY CALCULATION

The equation used to calculate the velocity of the fluid leaving the pump by use of the inverted manometer is presented here. All subscripts used should be referred to the figure below:

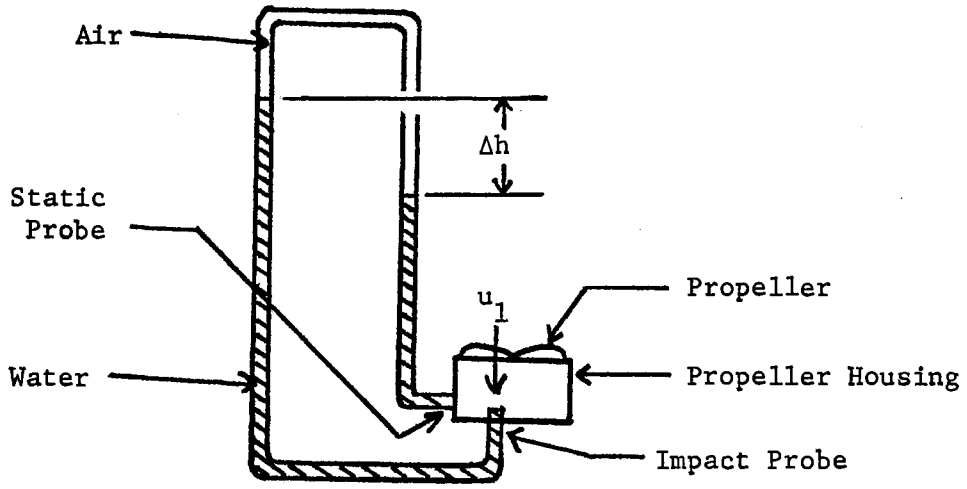

The steady, incompressible flow Bernoulli's equation is

$$P + \rho g y + \frac{1}{2} \rho u^2 = \text{constant} \qquad \text{(B-1)}$$

Hence, the velocity of the fluid leaving the pump, knowing the value of Δh from the manometer, is

$$u_1 = \left[\frac{2g(\rho_w - \rho_a)\Delta h}{\rho_w}\right]^{0.5} \qquad \text{(B-2)}$$

However, this equation can only be applied to situations where the

streamlines are straight. At higher propeller speeds, the propeller and shaft cause a rotation or swirl of the fluid, which leads to an additional pressure difference between the static probe and impact probe of the manometer. An estimate of the pressure change due to the rotation of the fluid can be calculated and the measured velocities corrected.

The velocity measured by the manometer is the perpendicular velocity of the flow. The tangential velocity of the flow can be estimated using trigonometry and is illustrated in the figure below.

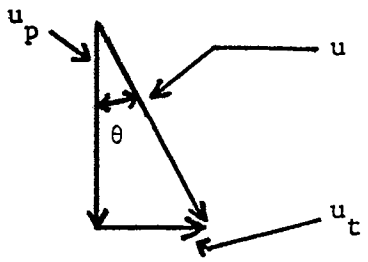

Attaching a string inside the propeller housing, the angle θ between the string and the perpendicular to the fluids surface was observed for a few propeller speeds and are tabulated below:

Revolutions per Second	Perpendicular Velocity	Angle
less than 2	less than 0.1 ft/sec	2°
3	0.1615 ft/sec	5°
14.7	1.053 ft/sec	25°

The angle never exceeded 30° for larger velocities. The calculated tangential velocities for the three perpendicular velocities used are:

$u_p = 1.053$ ft/sec $\quad u_t = 0.491$ ft/sec

$u_p = 0.1615$ ft/sec $\quad u_t = 0.0141$ ft/sec

$u_p = 0.05$ ft/sec $\quad u_t = 0.0017$ ft/sec

To estimate the change in pressure between the static and impact probe of the manometer a steady, two-dimensional, inviscid fluid flow is first assumed. Euler's steady-state equation normal to a streamline is

$$\frac{\partial P}{\partial n} = \frac{\rho U^2}{r} \tag{B-3}$$

For a helical flow, the projections of the flow are circles and the streamlines are concentric circles, and assuming the flow is incompressible, equation (B-3) can be written as

$$\frac{dP}{dr} = \frac{\rho U^2}{r} \tag{B-4}$$

or

$$dP = \frac{\rho U^2}{r}\, dr \tag{B-5}$$

If a solid-body type of rotation is assumed, then

$$U = r\omega \tag{B-6}$$

where ω is solid body angular velocity. Equation (B-5) can now be written as

$$dP = \frac{\rho r^2 \omega^2}{r}\, dr \tag{B-7}$$

and upon integrating equation (B-7) becomes

$$P_2 - P_1 = \left.\frac{\rho r^2 \omega^2}{2}\right|_1^2 \tag{B-8}$$

where point 1 will hereto be referred to the impact probes radial position and point 2 to the static probes radial position measured from the center of the circular propeller housing. The impact probe was placed 0.425 inches from the center of the propeller cowling and the related

geometry is illustrated below:

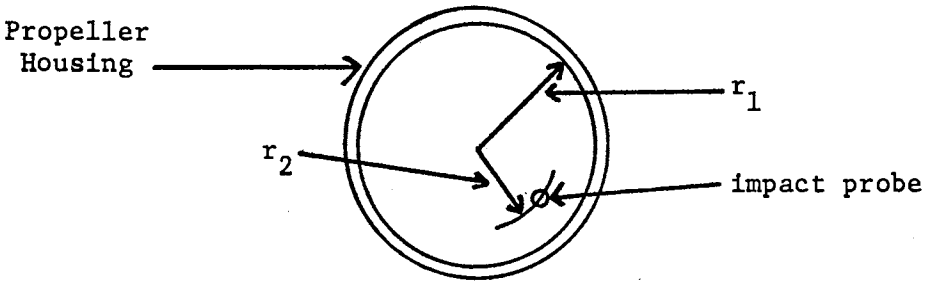

The angular velocity of the flow can be determined, with the use of equation (B-6), knowing the tangential velocity. Change in pressure between the impact probe and the static probe due to the rotation of the fluid can be calculated using equation (B-8). The change in pressure calculated due to the rotation of the fluid for each perpendicular velocity measured is:

$$u_p = 1.053 \text{ ft/sec} \qquad P_2 - P_1 = 0.0019 \text{ psi}$$

$$u_p = 0.1615 \text{ ft/sec} \qquad P_2 - P_1 = 1.6 \times 10^{-6} \text{ psi}$$

$$u_p = 0.05 \text{ ft/sec} \qquad P_2 - P_1 = 8.7 \times 10^{-8} \text{ psi}$$

Since an estimate of the change in pressure due to the rotation is known, the value of the velocity as measured by the manometer can be corrected. Equation (B-2) can also be written as

$$u = \left[\frac{2(P_2 - P_1)}{\rho_w}\right] 0.5 \qquad \text{(B-9)}$$

Knowing the velocity in equation (B-9), which is any one of the measured velocities, the pressure change which would be created by the change in velocity between the static and impact probes of the manometer can be calculated. This resultant pressure change can now be corrected by the amount of pressure difference created by the rotation of the fluid. The corrected pressure change can now be used, with equation (B-9), to calculate the corrected velocity. The values of the measured velocity and

the corrected velocities are

Measured	Corrected
1.053 ft/sec	0.92 ft/sec
0.1615 ft/sec	0.1608 ft/sec
0.05 ft/sec	0.05 ft/sec

As can be seen from the above figures, the effect of the rotation of the fluid at the low velocities is negligible, while at the higher velocities it cannot be neglected.

APPENDIX C

SURFACE DEPRESSION DUE TO VELOCITY

APPENDIX C

SURFACE DEPRESSION DUE TO VELOCITY

Due to the pumping of water downward, a surface depression will result. This surface disturbance must not reach the point at which air would be entrained in the propeller. Assuming that the fluid is inviscid, incompressible, and irrotational, the maximum surface depression will be estimated by use of Bernoulli's equation. Stator vanes placed above the propeller justify the assumption of irrotational flow. The following diagram will define the terms used in arriving at the estimate of the surface depression.

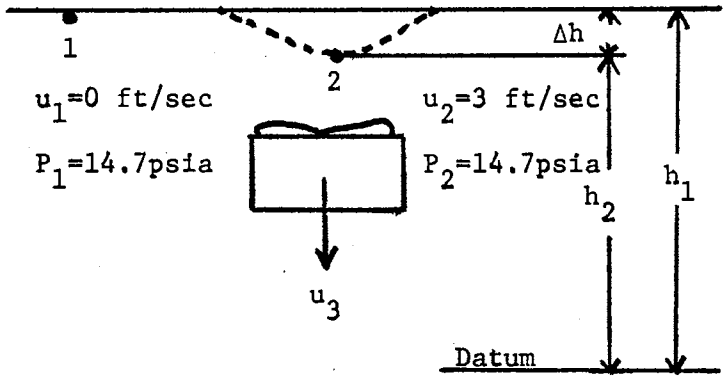

With these assumptions, Bernoulli's equation takes the form

$$P + \frac{1}{2}\rho u^2 + \rho g h/g_c = \text{constant} \qquad \text{(C-1)}$$

Since the maximum depression of the surface is desired, it is assumed

the velocity at point 2 is equal to the velocity at point 3. Both points 1 and 2 are vented to the atmosphere, therefore the static pressure at both points is atmospheric pressure. Knowing that Bernoulli's equation is equal to the same value at both points, the following equation can be written,

$$P_1 + \frac{1}{2}\rho u_1^2 + \frac{\rho g h_1}{g_c} = P_2 + \frac{1}{2}\rho u_2^2 + \frac{\rho g h_2}{g_c} \qquad \text{(C-2)}$$

but $p_1 = p_2$ and $u_1 = 0$, therefore

$$\Delta h = h_1 - h_2 = \frac{u_2^2}{2g} \qquad \text{(C-3)}$$

The propeller in the model is one and one-half inches below the surface and using this value as Δh would allow a velocity of two and one-half feet per second. The highest velocity used in this investigation was 1.294 feet per second, thus causing no problems with surface effects.

APPENDIX D

COMPUTER PROGRAM

APPENDIX D

COMPUTER PROGRAM

```
00   PRT "DENSITY IN"; PRT "OTHER UNITS FEET"' SPC 5
01   1 → X
02   ENT "HOW MANY DI YS. ?", RO
03   PRT "THE NUMBER OF"; PRT "DIVISIONS IS", RO
04   ENT "DIV CENT HG T = R1", R1
05   X + 1 → X; ENT "NEXT HEIGHT", RX; IF RO  X; GTO + 0
06   SPC 5; PRT "HEIGHTS OF DIV."; PRT "CENTERS ABOVE"; PRT "BOTTOM"
07   0 → X
08   X + 1 → X; PRT RX; IF RO > X; GTO + 0
09   ENT "RESP. AREAS = R51", R51
10   51 → X
11   X + 1 → X; ENT "NEXT AREA", RX; IF RO > X - 50; GTO + 0
12   SPC 5; PRT "AREAS"
13   50 → X
14   X + 1 → X; PRT RX; IF RO > X - 50; GTO + 0
15   2*R1 → R101; R101 → Y
16   100 → X
17   X + 1 → X; 2* (R(X - 99) - Y) → R (X + 1); Y + R (X + 1) → Y; IF
     RO > X - 100: GTO + 0
18   51 → X; R51 * R101 → R1 51; R151 → Y
19   X + 1 → X; RX*R (X + 50) → R (X + 100); R (X + 100) + Y → Y; IF
     RO > X - 50; GTO + 0
20   SPC 5; PRT "VOLUME OF"; PRT "DIVISIONS"
21   150 → X
22   X + 1 → X; PRT RX; IF RO > X - 150; GTO + 0
23   ENT "RESP. DENS. = R101", R101
24   101 → X
25   X + 1 → X; ENT "NEXT DENSITY", RS; IF RO > X - 100; GTO + 0
26   SPC 5; PRT "DENSITIES"
27   100 → X
28   X + 1 → X; PRT RX; IF RO > X - 100; GTO + 0
29   100 → X
30   X + 1 → X; RX*R (X + 50) → R (X - 50); IF RO > X - 100; GTO + 0
31   SPC 5; PRT "WEIGHT OF"; PRT "RESPECTIVE"; PRT "DIVISIONS"
32   50 → X
33   X + 1 → X; PRT RX; IF RO>X - 50; GTO + 0
34   51 → X
35   RX → B
36   X + 1 → X; RX + B → B; IF RO > X - 50; GTO + 0
37   1 → X
38   RX*R (X + 50) → A
```

```
39   X + 1 → X; RX*R (X + 50) + A → A; IF RO > X; GTO + 0
40   A/B → C; SPC 5
41   PRT "THE CENTER OF"; PRT "GRAVITY IS", C' PRT "FT ABOVE BOTTOM"
42   B/Y → R201; SPC 51
43   PRT "AVERAGE DENSITY", R201
44   C*B → R2021
45   SPC 5; PRT "THE POTENTIAL"; PRT "ENERGY OF THE"; PRT "LAKE IS",
     R202
46   R202*5. 05E - 7 → R203
47   SPC 1; PRT "OR"; SPC 1; PRT R203; PRT "HP-HRS"
48   SPC 5: GTO 1
49   STP
50   END R264
```

APPENDIX E

RICHARDSON NUMBER MATCHING

TABLE I

RICHARDSON NUMBER MATCHING--RECTANGULAR TANK VALUES

	Hamm's Lake Values	Model Values
$Ri_1 = -\frac{g\left(\frac{\partial \rho}{\partial z}\right)}{\rho_2\left(\frac{u}{h}\right)^2}$	$\frac{\partial \rho}{\partial z} = 0.01805$ lbm/ft^4 $\rho_2 = 62.3749$ lbm/ft^3 $u = 2.44$ ft/sec $h = 29.53$ ft $Ri_1 = 1.364$	$\frac{\partial \rho}{\partial z} = 2.022$ lbm/ft^4 $\rho_2 = 62.81$ lbm/ft^3 $h = 0.8631$ ft. Calculated velocity $= 0.7515$ ft/sec
$Ri_2 = -\frac{g\left(\frac{\partial \rho}{\partial z}\right)}{\rho_2\left(\frac{u}{w}\right)^2}$	$\frac{\partial \rho}{\partial z} = 0.01805$ lbm/ft^4 $\rho_2 = 62.3749$ lbm/ft^3 $u = 2.44$ ft/sec $w = 1275$ ft $Ri_2 = 2544.8883$	$\frac{\partial \rho}{\partial z} = 2.022$ lbm/ft^4 $\rho_2 = 62.81$ lbm/ft^3 $w = 3.548$ ft Calculated velocity $= 0.05126$ ft/sec
$Ri_3 = -\frac{g\left(\frac{\partial \rho}{\partial z}\right)}{\rho_2\left(\frac{vol}{\dot{vol}}\right)^2}$	$\frac{\partial \rho}{\partial z} = 0.01805$ lbm/ft^4 $\rho_2 = 62.3749$ lbm/ft^3 $v = 40{,}030{,}000$ ft^3 $\dot{v} = 23.47$ $Ri_3 = 2.710 \times 10^{10}$	$\frac{\partial \rho}{\partial z} = 2.022$ lbm/ft^4 $\rho_2 = 62.81$ lbm/ft^3 $v = 39.65$ ft^3 area $= 0.008522$ ft^2 Calculated velocity $= 0.02877$ ft/sec

TABLE II

RICHARDSON NUMBER MATCHING--CONTOUR VALUES

	Experiment 1	Experiment 2	Experiment 3
	$\rho_2 = 63.9725$ lbm/ft^3	$\rho_2 = 63.8539$ lbm/ft^3	$\rho_2 = 63.9038$ lbm/ft^3
	$(\partial\rho/\partial z) = 4.04$ lbm/ft^4	$(\partial\rho/\partial z) = 5.24$ lbm/ft^4	$(\partial\rho/\partial z) = 4.48$ lbm/ft^4
	$h = 0.86$ ft	$h = 0.86$ ft	$h = 0.86$ ft
	$w = 3.55$ ft	$w = 3.55$ ft	$w = 3.55$ ft
	$v = 12.29$ ft^3	$v = 12.29$ ft^3	$v = 12.29$ ft^3
	$\dot{v} = 0.009$ ft^3/sec	$\dot{v} = 0.0012$ ft^3/sec	$\dot{v} = 0.00043$ ft^3/sec
	$u_1 = 1.053$ ft/sec	$u_2 = 0.1615$ ft/sec	$u_3 = 0.05$ ft/sec
$Ri_1 = -\frac{g(\partial\rho/\partial z)}{\rho_2(u/h)^2}$	Ri_1 at u_1 $Ri_{11} = 1.36$	Ri_1 at u_2 $Ri_{12} = 74.9$	Ri_1 at u_3 $Ri_{13} = 667$
$Ri_2 = -\frac{g(\partial\rho/\partial z)}{\rho_2(u/w)^2}$	Ri_2 at u_1 $Ri_{21} = 23.1$	Ri_2 at u_2 $Ri_{22} = 1{,}280$	Ri_2 at u_3 $Ri_{23} = 11{,}400$
$Ri_3 = -\frac{g(\partial\rho/\partial z)}{\rho_2(\dot{v}/v)^2}$	Ri_3 at u_1 $Ri_{31} = 3.79\times10^6$	Ri_3 at u_2 $Ri_{32} = 2.77\times10^8$	Ri_3 at u_3 $Ri_{33} = 1.84\times10^9$

APPENDIX F

POTENTIAL ENERGY CURVES

APPENDIX F

POTENTIAL ENERGY CURVES

The potential energy curves presented in this appendix represent the theoretical amount of energy needed to destratify the lake or model as a function of time. As was discussed in Chapter IV, the amount of energy needed to destratify a lake can be calculated, but this value would only be the theoretical value. Due to inefficiencies, more energy would actually be required to destratify the lake. The first point on the curve is the theoretical amount of energy needed to destratify the lake with the lake in a stratified condition. At a given time later, the lake will have been destratified to some extent, but the energy required to destratify the lake to this new condition will be more than the theoretical amount because of inefficiencies. A new theoretical amount of energy needed to destratify the lake can now be calculated. Through this process, the curves presented in this appendix have been plotted.

The curve for the model shows a resemblance to an exponential curve. The curve for Hamm's lake was divided into two sections. The data available from Hamm's lake was taken at irregular intervals. The warming of the sun or the cooling of the lake in the evening caused temperature profiles near the surface to vary from morning to evening. By separating data taken in the morning and evening, more uniform curves were obtained. With all data points plotted together, a random

distribution occurs. The last three data points of the morning curves in two cases resemble exponential curves. A more complete set of data from a destratification project on a real lake would be necessary to determine if potential energy curves would prove useful in modeling lake destratification. The potential energy curves are presented in Figures 24 and 25.

APPENDIX G

ERROR ANALYSIS

APPENDIX G

ERROR ANALYSIS

This error analysis is intended to provide an estimate of the accuracy to which the velocity leaving the pumping device can be determined. Neglecting swirl for the moment, the velocity is calculated using equation (B-2),

$$u = \frac{2g(\rho_w - \rho_a)\Delta h}{\rho_w}^{0.5}$$

This is the equation shown in Appendix B. In the experiments conducted, all the terms on the right hand side of equation (B-2) will remain constant except Δh. Therefore

$$u \sim (\Delta h)^{0.5} \tag{G-1}$$

Taking the natural logarithm of both sides and differentiating gives

$$\ln u \sim \ln(\Delta h^{0.5}) \tag{G-2}$$

$$\ln u \sim \tfrac{1}{2}\ln(\Delta h) \tag{G-3}$$

$$\frac{du}{u} \sim \tfrac{1}{2}\frac{d(\Delta h)}{\Delta h} \tag{G-4}$$

If it is assumed that the variations or changes in the velocity and Δh readings are small, equation (G-4) can be written as

$$\frac{\Delta u}{u} = \tfrac{1}{2}\frac{\Delta(\Delta h)}{\Delta h} \tag{G-5}$$

an estimate of the percentage error in the velocity can be determined from equation (G-5) and is equal to one-half the percentage uncertainty in the reading of Δh.

With the use of a magnifying lens and a marker graduated in 0.02 inch increments, the value of Δh could be read to within 0.01 inch. The smaller the value of Δh read from the manometer, the larger the percentage error in the velocity. Because it was necessary to use velocities with corresponding small Δh, large errors were encountered. The calculated errors for each measured velocity obtained by the above procedure are presented below with the associated velocity:

u=1.053 ft/sec	error=2.4 percent
u=0.1615 ft/sec	error=81 percent
u=0.05 ft/sec	error-1072 percent

A more accurate method to determine the smaller velocities is to find the relationship between the shaft rotation and the velocity. An equation of the following form was assumed to describe the relationship between the shaft rotation and velocity,

$$u=k(r^b). \qquad \text{(G-6)}$$

Measurements of Δh were made two separate times for several values of propeller rotation and the corresponding velocity was calculated using equation (B-2). The resultant values are presented below:

RPS	Δh(inches)	Velocity(ft/sec)	Δh(inches)	Velocity(ft/sec)
5	0.02	0.3274	0.02	0.3274
10	0.08	0.6548	0.08	0.6548
15	0.24	1.134	0.26	1.181
20	0.42	1.500	0.45	1.553
25	0.69	1.923	0.75	2.005
30	1.59	2.919	1.42	2.759

Using values of shaft rotation and velocity from the preceding figures,

the constants k and b can be calculated. The resulting equation is

$$u=0.0469\ r^{1.2}. \tag{G-7}$$

An uncertainty band has been added to Figure 10 in Appendix A with the use of equation (G-7). The error in the velocities will be estimated using the uncertainty bands on Figure 10. The error for the velocities of 1.053 ft/sec, 0.1615 ft/sec, and 0.05 ft/sec are respectively 9.2 percent, 8.4 percent, and 10 percent.

The primary parameter is the Richardson number and the error in the Richardson number will be a function of the error in each individual term. The Richardson number can be written as

$$Ri= - \frac{g(\frac{\Delta\rho}{z_1})}{\rho_2(\frac{u}{z_2})^2} \tag{G-8}$$

or

$$Ri= - \frac{g\Delta\rho z_2^2}{\rho_2 u^2 z_1} \tag{G-9}$$

where the z terms are the values such as height or width for the three Richardson numbers used. Following the same procedure as used for equation (G-1), the error in the Richardson number can be written as,

$$\frac{\Delta Ri}{Ri} = \frac{\Delta g}{g} + \frac{\Delta(\Delta\rho)}{\Delta\rho} + 2\frac{\Delta z_2}{z_2} - \frac{\Delta\rho_2}{\rho_2} - 2\frac{\Delta u}{u} - \frac{\Delta z_1}{z_1} \tag{G-10}$$

Since it is not known whether the changes are positive or negative, the maximum error in the Richardson number would be the sum of the absolute values of each term. The total error in the Richardson number can now be calculated when the error in each individual term is determined.

It is assumed that the value used for the gravitational constant is correct and no error exists in this term. The z_1 term, the depth over which the maximum change in density was measured, was always one-half inch. The accuracy to which this could be measured was one-thirty-second of an inch, producing an error in the z_1 term of 6.3 percent. The error in z_2, where z_2 is equivalent to the lake height in Ri_1 and the lake width in Ri_2, can be determined by dividing the accuracy to which the measurement can be made by the measurement. The errors for Ri_1 and Ri_2 respectively are 0.8 percent and 2.4 percent.

When the theoretical value of density for a known amount of salt in a known volume of water was compared to the value of density as measured by the conductivity probe, the maximum difference in specific gravity between any two measurements was 0.0006. This value will be used as the uncertainty in the measured values of density. The accuracy of the $\Delta\rho$ term is the sum of the error in each density measurement divided by the difference in the density measurement. The error in ρ_2 is simply the accuracy of the measurement divided by the measurement. The error in the ρ_2 term for Ri_1, Ri_2, and Ri_3 is 0.06 percent and the error in the $\Delta\rho$ term for Ri_1, Ri_2, and Ri_3 are respectively 5 percent, 5.4 percent, and 5.2 percent. Since Ri_3 used a term of volume flow rate divided by volume, the error in these terms will be the accuracy of the measured velocity and the accuracy of the measurement of the volume divided by the volume. The error in the volume flow rate is 10 percent and the error in the volume is 5 percent.

An estimated total maximum error can now be calculated for each Richardson number with the use of equation (G-10) and the errors calculated for each term. The following values of error were calculated,

Error in Ri_1 = 31 percent

Error in Ri_2 = 33 percent

Error in Ri_3 = 35 percent

The uncertainty in the calculation of the non-dimensional time for complete destratification of the model can also be made. The procedure used for equation (G-1) is again used here to derive the expression required to determine the uncertainty in τ. The final form is

$$\frac{\Delta\tau}{\tau} = \frac{\Delta t}{t} + \frac{\Delta\dot{v}}{\dot{v}} + \frac{\Delta v}{v} \qquad \text{(G-11)}$$

where the uncertainty in $\dot{v}$ and v are 10 percent and 5 percent respectively. The uncertainty in t is the recording time increments divided by the total time required for destratification. For Ri_1, the uncertainty in t is 33 percent and the total uncertainty in τ is 44 percent. For Ri_2, the uncertainty in t is 3 percent and the total uncertainty in τ is 12 percent. Since the model did not destratify with Ri_3 as the non-dimensional parameter, τ would be infinite.

VITA

Thomas Alan Gibson

Candidate for the Degree of

Master of Science

Thesis: INVESTIGATION OF ARTIFICIAL LAKE DESTRATIFICATION--A HYDRAULIC MODEL STUDY

Major Field: Mechanical Engineering

Biographical:

Personal Data: Born in Oklahoma City, Oklahoma, June 12, 1949, the son of Mr. and Mrs. Joe F. Gibson.

Education: Graduated from Northwest Classen High School, Oklahoma City, Oklahoma, in May, 1968; received Bachelor of Science degree in Mechanical Engineering from Oklahoma State University in 1972; completed requirements for the Master of Science degree at Oklahoma State University in July, 1974.

Professional Experience: Engineer-in-training; Member of American Society of Mechanical Engineers; graduate research assistant, School of Mechanical and Aerospace Engineering, Oklahoma State University, 1973-74.